Geological Society of America
Special Paper 405
2006

The 3.466 Ga "Kitty's Gap Chert," an early Archean microbial ecosystem

Frances Westall[†]
Centre de Biophysique Moléculaire, CNRS, Rue Charles Sadron, 45071 Orléans cedex 2, France
Sjoukje T. de Vries[‡]
Wouter Nijman[§]
Faculty of Geosciences, Utrecht University, Budapestlaan 4, 3584 CD Utrecht, The Netherlands
Virgile Rouchon[#]
Département des Sciences de la Terre, UMR CNRS-UPS Interaction and Dynamics of Surface Environments, Université Paris Sud, Bât. 504, 91405 Orsay Cedex, France and
Planetary Science Laboratory, Osaka University, 1-1 Machikaneyama, Toyonaka, 560-0043 Osaka, Japan
Beate Orberger[††]
Département des Sciences de la Terre, UMR CNRS-UPS Interaction and Dynamics of Surface Environments, Université Paris Sud, Bât. 504, 91405 Orsay Cedex, France
Victoria Pearson[‡‡]
Jon Watson[§§]
Alexander Verchovsky[##]
Ian Wright[†††]
Planetary and Space Sciences Research Institute (PSSRI), The Open University, Walton Hall, Milton Keynes, K7 6AA, UK
Jean-Noël Rouzaud[‡‡‡]
Centre de la Matière Divisée, CNRS, 1B rue de la Férollerie, 45071 Orléans cedex 2, France
Daniele Marchesini[§§§]
via Torino 10, 40139 Bologna, Italy
Anne Severine[###]
Department of Geological Sciences, University of Orléans, 45071 Orléans cedex 2, France

[†]E-mail: westall@cnrs-orleans.fr.
[‡]E-mail: stdevries@geo.uu.nl.
[§]E-mail: wnijman@terra.geo.uu.nl.
[#]E-mail: rouchon@geol.u-psud.fr.
[††]E-mail: orberger@geol.u-psud.fr.
[‡‡]E-mail: v.k.pearson@open.acuk.
[§§]E-mail: j.watson@open.ac.uk.
[##]E-mail: a.verchovsky@open.ac.uk.
[†††]E-mail: i.p.wright@open.ac.uk.
[‡‡‡]Present address: Laboratoire de Géologie, Ecole Normale Supérieure de Paris, 24 rue Lhomond, 75231 Paris Cedex 5, France; e-mail: rouzaud@mailhost.geologie.ens.fr.
[§§§]E-mail: danilel@tin.it.
[###]E-mail: anne.severine@free.fr.

Westall, F., de Vries, S.T., Nijman, W., Rouchon, V., Orberger, B., Pearson, V., Watson, J., Verchovsky, A., Wright, I., Rouzaud, J.-N., Marchesini, D., and Severine, A., 2006, The 3.466 Ga "Kitty's Gap Chert," an early Archean microbial ecosystem, *in* Reimold, W.U., and Gibson, R.L., Processes on the Early Earth: Geological Society of America Special Paper 405, p. 105–131, doi: 10.1130/2006.2405(07).

ABSTRACT

A multidisciplinary study of silicified volcanoclastic, near-shore deposits from the 3.446 Ga "Kitty's Gap Chert," Warrawoona Group, Pilbara, reveals that they contain a wealth of carbonaceous microbial fossil remains. The volcanoclastic sediments host predominantly colonies of coccoidal microorganisms that occur in two modal size ranges, 0.4–0.5 μm and 0.75–0.8 μm. These microbial colonies coat the surfaces of the volcanic particles and form either dense, carpetlike associations up to tens of micrometers in diameter comprising hundreds of individuals. They also form less dense concentrations that include many chainlike associations of coccoids. All colonies are associated with a polymer film (extracellular polymeric substances—EPS) that coats both the organisms and their substrate. Multispecies biofilms formed at a boundary representing a short period of nondeposition. They consisted predominantly of coccoids and EPS but also included common, small filaments tens of micrometers in length and 0.25 μm in width and rare, short rods 1 μm in length. Carbon isotopic compositions of about –26‰ to –30‰, measured on individual layers, are compatible with microbial fractionation. The biofilms include possible anoxygenic-photosynthesizing organisms (the filaments), whereas the colonies coating the volcanic clasts probably represent chemolithotrophic organisms. The interaction between the microbes, their colonies and biofilms, and their environment is intimate and complex. The environment provided the substrate and the nutrient, energy, and carbon sources, whereas the metabolic activity of the microbes contributed to the early diagenetic alteration of the volcanic particles, to the binding of the sediment, and to their silicification. The microorganisms were preserved by rapid silicification, with the silica coming partly from hydrothermal sources and partly from pore water enrichment in Si due to the devitrification of the volcanic protoliths (partially mediated by microbial activity).

Our multidisciplinary approach to the study of this sample demonstrates the importance of using complementary methods in order to understand the complex microbe/sediment interactions and to be able to relate different types of microbial colonies/biofilms to different microenvironments. The observations and conclusions from this study have important consequences for the methods that need to be used in the search for traces of past life in general and especially in the search for past life on other planets such as Mars.

Keywords: Archean, "Kitty's Gap Chert," near-shore environment, microfossil, anoxia, chemolithotroph, anoxygenic photosynthesizer.

INTRODUCTION

Given the complex interactions of microorganisms with their environment, we have approached the study of fossil microorganisms and biofilms using a variety of methods (Westall, 2005a), ranging from (1) macroscopic to microscopic interpretation of the ecologic environment, (2) optical microscope and geochemical characterization of the composition of the primary sedimentary material, as well as of the early diagenetic and metamorphic changes that took place, (3) optical and high-resolution scanning electron microscope characterization of the microfossil remains, (4) high-resolution transmission electron microscope study, Raman spectroscopy, and isotopic investigations of the organic carbon remains, and (5) nuclear microprobe and isotopic investigation of nitrogen, trapped as a chemical fossil in mica minerals (Rouchon et al., 2005). This multidisciplinary approach has allowed us to (1) make detailed interpretations of the macro- and microenvironment, (2) conclude that the microstructures observed have a high probability of biogenicity, and (3) understand the early diagenetic and metamorphic history of the rock.

The variety of methods that we have adopted is essential in providing an acceptable level of confidence for the interpretation of potentially biogenic structures in these ancient sediments, especially given the recent discussions concerning the identification of microbial fossils and the origin (biogenic or abiogenic) of the organic carbon in early Archean cherts (Brasier et al., 2002; van Zuilen et al., 2002, 2003; Westall, 2004) or in Martian meteorites (McKay et al., 1996; Cady et al., 2003). The silicified volcano-sedimentary sequences of the early Archean terrains in

the Pilbara in northwestern Australia and also in Barberton in South Africa are the oldest, well-preserved sediments known to date. Although older sediments (3.65–3.85 Ga) occur in southwestern Greenland (McGregor and Mason, 1977; Fedo, 2000; Rosing, 1999), amphibolite to granulite facies metamorphism has so altered the original texture and mineralogy of these rocks that they cannot be used for microfossil study. In fact, the microfossils that had been described, e.g., by Pflug (1979, 2001), Pflug and Jaeschke-Boyer (1979), and Robbins (1987), have been reinterpreted as recent endolithic contaminants (Westall and Folk, 2003). The sediments from the Pilbara and Barberton regions are therefore the oldest rocks that can be used in the search for fossilized traces of ancient life. A number of investigations of microfossils in Pilbara rocks have been previously made (see Schopf and Walter, 1983 and references therein; Schopf and Packer, 1987; Schopf, 1993; Hofmann et al., 1999; Schopf et al., 2002; Allwood et al., 2005a, 2005b). However, many of the biogenic interpretations of individual structures as fossilized cyanobacteria, of domical stromatoloids as microbial stromatolites, and even of the negative values of carbon isotopes that are usually taken as indicators of biogenic processes, have been questioned (e.g., Buick, 1990; Lowe, 1994; Brasier et al., 2002; van Zuilen et al., 2002). In the light of these discussions and given the submicrometer- to micrometer-scale nature of the individual microbial structures preserved within the early Archean cherts from the Pilbara, we believe that an investigation integrating observations and analyses on a meter to submicrometer scale is both necessary and realistic in order to reliably study potential microfossils and their biofilms in situ in ancient sediments. In this study we therefore make special use of high-resolution scanning electron microscopy, coupled with light element analysis (EDX), to reveal the wealth of detail and information that is trapped within the cherts and that cannot be obtained by the traditional, optical microscope methods that have previously been used in the search for Archean microfossils.

Microorganisms and Biofilms

Microorganisms in nature do not occur in isolation; they form colonies, often consisting of multispecies consortia as well as biofilms and mats. The term "biofilm" usually refers to a laterally extensive development of microbial colonies encased in a polymer matrix of extracellular polymeric substances (EPS), whereas "microbial mat" refers to a generally well-developed biofilm that includes both trapped detrital particles and authigenically precipitated minerals. The terms are, however, used interchangeably (Levitt and Krumbein, 2003). Individual microbial colonies can form on any kind of substrate and do not necessarily form biofilms or mats. The relationship between the microorganisms and their substrate is complex; the substrate provides a support for the microbial colony and also serves as a source of energy and nutrients (Madigan et al., 2000). Microbes can take advantage of redox reactions occurring at the surface of reactive particles, such as minerals and volcanoclastic material, that provide the electrons necessary for driving their energetic metabolic processes and, consequently, biosynthesis. Such microorganisms are known as chemolithotrophs; they obtain both their energy and their carbon from inorganic sources, whereby the carbon comes from CO_2 (autotrophy), organic compounds that are readily biodegradable, or organic molecules (mixotrophy). Alteration of the particles (often through the corrosive action of excreted microbial metabolites) liberates the essential elements (macronutrients) that the microorganisms require, such as N, P, S, Mg, K, Ca, Na, and Fe, as well as metallic micronutrients (including Fe, Cr, Co, Cu, Mn, Mo, Ni, Si, W, V, and Zn). Thus, diagenetic alteration of mineral or volcanic surfaces exposed to seawater, including the pore waters of volcanic sediments, can be regarded as a combination of microbial and physicochemical processes acting on the particles.

Biofilms and microbial mats are architecturally complex structures (Charaklis and Wilderer, 1989) that can also be compositionally heterogeneous, consisting of a variety of cohabiting microorganisms that form a consortium. The biofilm structure is advantageous to the organisms because (1) the water-rich polymer film provides them with protection, especially in severe environmental situations, (2) within the biofilm, microorganisms can create their own microenvironment with controlled redox and pH conditions and nutrient concentrations, and (3) the different organisms within a biofilm are complementary and not necessarily in competition with each other; each organism is specialized such that what one organism excretes as a metabolite, another can use as a nutrient. Moreover, the different types of organisms obtain their energy and carbon sources in different ways that are not necessarily in competition with each other.

Biofilms interact with their substrate in a variety of ways such as sediment stabilization and/or lithification. The exopolymeric substances (EPS) are cohesive polymers that bind or cement sediment particles together (Krumbein et al., 1994; Westall and Rincé, 1994). The physical expression of the films can be delicate or they can be very thick and robust, depending on the time available for development or the environment of development. These films can form very rapidly in ephemeral environments, such as tidal mud flats (Stal, 1994). Colonies of microbes, biofilms, and mats are heavily implicated in the lithification of sediments (Krumbein et al., 1994). The EPS as well as the envelopes around the individual microorganisms are rich in reactive functional groups, such as hydroxyls, phosphoryls, and carboxyls, that readily complex metal ions (Monty et al., 1991; Westall et al., 1995). Depending on the availability of metal ions and suitable physical conditions, ions such as Si, Fe, or Ca (among others) form a complex with the functional groups of the organic substrate, then polymerize, thus acting as a chemical fixative and fossilizing agent. Therefore, although microbes and their biofilms may be ephemeral on geological time scales, they have the potential of being rapidly preserved and, thus, the potential to pass into the geological record.

Apart from the differences in temporal scales between microbial and geological phenomena, microbial spatial scales are also orders of magnitude smaller than geological spatial scales. Individual microbes are of the order of some hundreds of nanometers to several micrometers in size, depending on the species (and some filaments are >100 μm in length). [*N.B.* Most microbial organisms in nature are smaller in size than those in a laboratory culture.] Microbial colonies may consist of a few to very many ($\geq 10^3$) individuals and cover areas ranging from a few to many hundreds of micrometers in diameter. Microbial biofilms or mats, on the other hand, are generally much larger, of the order of hundreds of μm^2 to m^2 and even up to km^2 in dimension.

When studying the fossilized remains of microbes, colonies of microbes, and their biofilms and mats in rocks, account needs to be taken of the effects of the differences in spatial and time scales on quantification of the microbes in a rock (and therefore on elemental concentrations such as organic C, N, and S, as well as the isotopic ratios of these elements). Although microbes and their biofilms may appear to be relatively common in sediments, their volumetric importance may be insignificant with respect to that of the bulk sediment. Biomass development depends upon variables such as environmental conditions including nutrient availability, pH, and salt concentrations, as well as on metabolic pathway. In the shallow water environment studied, the organisms and their biofilms are surface specific: they may be common in one microenvironment (on a scale of 10^{1-3} μm) but not in the adjacent environment. Thus, although a rock may be locally enriched in microbial remains (and C, N, and S) on a scale of 10^{1-3} μm, the bulk sample may contain only small quantities of these components.

Geological Setting of the "Kitty's Gap Chert"

The object of this study is a chert formation, here called the "Kitty's Gap Chert," that is part of the Panorama Formation in the Warrawoona Group and outcrops 50 km northeast of the town of Marble Bar in the Coppin Gap Greenstone Belt, Pilbara, northwestern Australia (Fig. 1) (Hickman, 1983, 1990; DiMarco and Lowe, 1989; Eriksson et al., 1994; Van Kranendonk et al., 2002). Dating of a felsic unit in the formation shows it to be 3.445 ± 4 Ga (de Vries, 2004) and therefore the lateral equivalent of the Panorama Formation in the North Pole Dome area (cf. also Williams, 1990). It consists of a series of packets of silicified volanoclastic sediments (Fig. 2) that were deposited in a near-shore, channel-and-flat environment. Each packet of sediments is separated by material of more mafic nature (de Vries, 2004). The cherts are underlain by rhyolitic and dacitic-rhyolitic volcanics and overlain by basalt. The whole volcano-sedimentary complex of the Panorama Formation was deposited in a large basinal structure characterized by growth faults (Nijman et al., 1999; de Vries, 2004). Silica-rich hydrothermal fluids used this fracture system as a conduit to the surface (Fig. 1). At the sample location, a hydrothermal silica vein penetrates into the lowermost layer of the silicified volcanoclastic sediments, fracturing them and dissipating laterally into

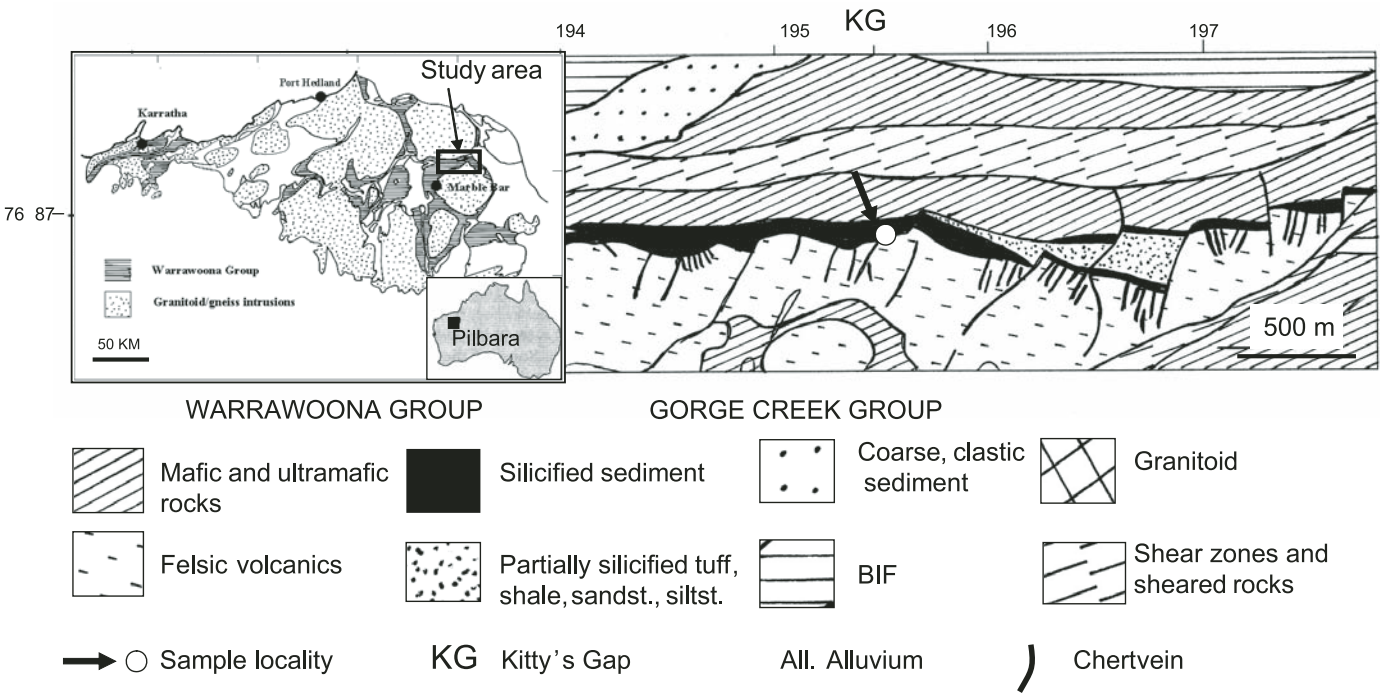

Figure 1. Pilbara study area location and detailed geological map of Kitty's Gap volcano-sedimentary sequence (after de Vries, 2004). Coordinates refer to Australian map grid zone 51.

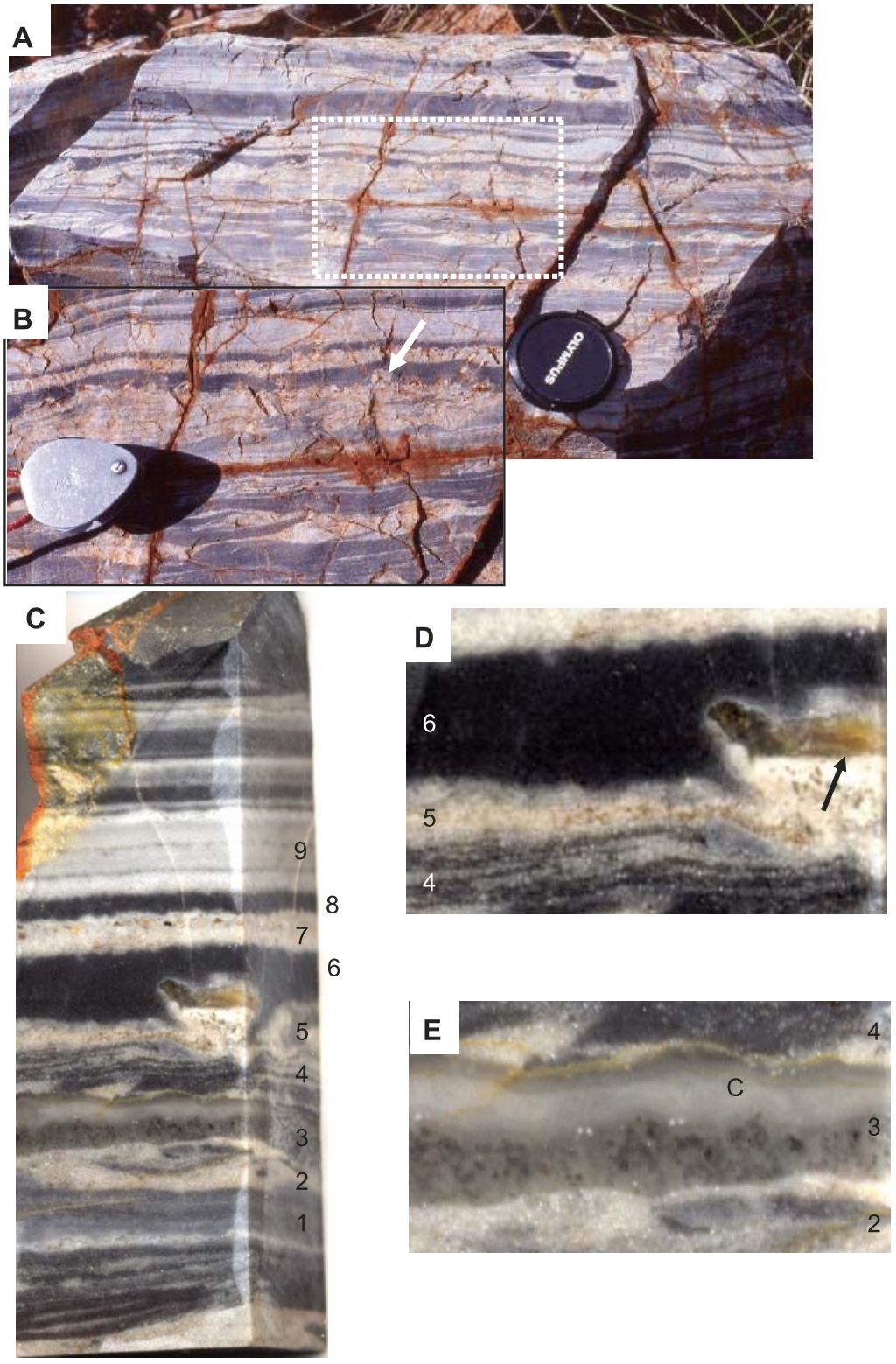

Figure 2. (A, B) Field view of silicified, near-shore channel-and-flat, volcanoclastic sediments that are the subject of this study. Scale—lens cap 5.4 cm. (B). Detail of flaser-linsen and cross-bedding structures, as well as the layer (Layer 5) embedded pumice fragments (arrow). Scale—hand lens 3.5 cm long. (C, D, E) Cut surface of rock showing different layers, 1–9, described in the text. (D) Detail of Layers 5 and 6. Note clear horizontal distinction between lower, more silicified part of pumice fragment and upper, translucent, hydromuscovite-rich part (arrow). This boundary is in lateral continuation with the top of Layer 5. (E) Detail of Layer 3 highlighting a lower, speckled stratum consisting of silicified, Ti oxide-rich volcanic particles, and an upper, translucent stratum of chalcedony (C) that precipitated probably in an open crack during early diagenesis.

them. The influence of the disruptive pressure of the hydrothermal fluids decreases laterally along the sediment layers with distance from the chert vein. The silicified sediments now outcrop as an east-west oriented ridge, in which the volcanosedimentary layers are dipping vertically or are slightly overturned. The rocks underwent burial metamorphism up to the upper stages of the prehnite-pumpellyite facies (Kisch and Nijman, 2004).

MATERIALS AND METHODS

Sample

The sample studied was obtained from the lowermost layer of the "Kitty's Gap Chert," immediately overlying the felsic volcanics (sample location coordinates: 0195366E; 7686751S (the grid numbers refer to Australian map grid zone 51) [120°04.53′E; 20°53.62′S] (Fig. 1). This sample was chosen because the field exposure of the silicified volcanoclastics exhibited an intriguing, laterally continuous horizon (over a scale of several meters) characterized by small lumps of the order of 0.5 cm in size on the top of ripple-marked sediments (Fig. 2). Subsequent analysis showed that the "lumps" were, in fact, pieces of silicified pumice and that a delicate microbial mat had formed at the top of the surface of ripple-marked sediments and pumice fragments. Two samples of this horizon were taken, one ~2 m east of the chert vein and one further away from the vein at a distance of 1 m from the previous sample (i.e., 3 m from the vein).

Sedimentologic and Mineralogic Characterization

Careful field characterization at the outcrop level of the formation was undertaken in order to understand the geological and environmental context of the deposit (de Vries, 2004). Further information concerning the fine-scale sedimentological environment and composition of the particles came from optical and scanning electron microscope study of the cut rock surface and thin sections. The microscopes used included an Olympus BX51 optical microscope and a Jeol FEG [field emission scanning electron microscope] SEM 6400 (NASA–Johnson Space Center, Houston) and a Hitachi FEG SEM S4200 (University of Orléans) as scanning electron microscopes.

Geochemical Characterization

Two Cameca SX50 electron microprobes (at the BRGM [Bureau de la Recherché Géologique et Minéralogique], Orléans and Centre Camparis, Université Paris VI) were used for major, minor, and trace element analyses in minerals. Working conditions at the BRGM–Orléans were: acceleration voltage 15 kV, beam current 12nA, and beam width 1 μm^2. The standards used included: K—orthoclase ($KAlSi_3O_8$), Ti—MnTiO3 (synthetic), Fe—hematite (Fe_2O_3), Na—albite ($NaAlSi_3O_8$), Ca—andradite ($Ca_3Fe_2Si_3O_{12}$), Cl—vanadinite ($Pb_5(VO_4)_3Cl$), Cu—Cu metal, Si—albite ($NaAlSi_3O_8$), S—barytes ($BaSO_4$), U—UO_2, Cr—Cr_2O_3 (synthetic), Al—corundum (Al_2O_3), V—vanadinite ($Pb_5(VO_4)_3Cl$), Mg—olivine $(Mg,Fe)_2SiO_4$. Working conditions for the Cameca SX50 at the Centre Camparis, Université Paris VI, are described in Orberger et al. (this volume). The nuclear microprobe (nuclear reaction analyses (NRA) of the Laboratoire Pierre Süe (CEA–CNRS [Commisariat à l'Enérgie Atomique]) was used to locate C and N in minerals (Rouchon et al., 2005). Further details related to the in-depth geochemical investigations (electron and nuclear microprobes, ICP-AEX [inductively-coupled plasma atomic emission spectrometry] and ICP-MS [inductively-coupled plasma mass spectrometry]) are given in Orberger et al. (this volume) and Rouchon et al. (2005).

Organic Carbon/Nitrogen Investigations

High-Resolution Transmission Electron Microscopy (TEM)

For the high-resolution transmission electron microscope study of the carbonaceous component of the sample, a small portion of the pumice layer horizon with the biofilm and a small portion of the underlying layer of ripple-marked volcanoclastic sediments were digested in HF and HCl to eliminate the mineral fraction. A small drop of the residue in suspension in alcohol was deposited on a prepared lacey TEM grid and observed with a Philips CM20 instrument fitted with an energy-dispersive spectrometer (EDX system). The (002) lattice fringe mode of observation allows the direct imaging of the polyaromatic layers forming the skeleton of carbon materials (Boulmier et al., 1982; Oberlin, 1989; Rouzaud and Clinard, 2002).

Raman Spectroscopy

Raman spectroscopy (DILOR XY800) was performed on the same layers in the cut surface of the sample to obtain information on the maturity of the carbonaceous material. The working conditions were as follows: excitation provided by a green beam at 514.5 nm by an Ar Coherent Radiation laser; multichannel detector DDd WRIGHT; objective: MDPLAN Olympus ×100; acquisition rates of 50–300 s with a final power value of 0.4–1mW.

Bulk Carbon Analysis and Carbon Isotope Analysis

Carbon concentrations and isotopic composition were measured on bulk samples of individual layers at the Open University by stepped combustion (from 200 to 1400 °C with 100 increments) using a static mode machine MS-86 (Wright and Pillinger, 1989; Verchovsky et al., 2002). The system blank was ~10 ng and the precision for $\delta^{13}C$ is ± 1‰. The samples were crushed to ~0.1 mm grain size before analysis, and aliquots with weights from 2 to 22 mg were used. In one case (Layer 7) we also analyzed an uncrushed sample. In the experiment, the carbon yield was also measured. The system blank was ~5 ng of C.

Microfossil Investigations

Sample Preparation

Preliminary identification of a potential microbial biofilm at the pumice layer surface was made in thin section. For high-resolution scanning electron microscope study, a number of preparations of the sample taken furthest away from the intruding chert vein were made to ensure reproducibility and to ensure that the microstructures studied were in situ and formed contemporaneously with sediment deposition (i.e., endogenous). These preparations included a raw, freshly broken surface, a polished thin-section surface, and a simple cut surface. The preparations were cleaned in milliQ water in an ultrasonic bath, dried, and then dipped in alcohol and flamed to eliminate surface contamination. Some of the specimens were delicately etched in the fumes of HF for 1 h. The etched preparations were then abundantly rinsed in milliQ water before being dried and coated with either Au or Au/Pt for SEM observation. The SEMs used are those listed above (a Jeol FEG SEM 6400 and a Hitachi FEG SEM S4200). All the instruments were equipped with a light element EDX detector that was used to make qualitative spot analyses of the elemental composition, as well as maps of various elements, especially C, associated with specific microstructures. Observations were made in secondary as well as backscattered electron mode. Most of the microfossil observations were made on the etched cut sample surface, and others were made on the thin-section surface.

Microfossil Identification

The identification of the microfossils was based on two main aspects: (1) compatibility of the environment of deposition with the existence of living organisms, and (2) demonstration of characteristics indicative of biogenicity. We recognize that there is no one observation or measurement that, on its own, is proof of biogenicity. Rather, many lines of evidence need to be assembled to arrive at a probability of biogenicity. The probability of biogenicity can be expressed in many ways, for instance as a number (e.g., from one to five with increasing confidence of biogenicity) or in terms of adjectives (e.g., strong, moderate, weak).

The criteria indicative of biogenicity used in this study are related to the structural and biogeochemical aspects of an organism. These criteria will vary depending on the species of microorganism. For example, the morphological criteria used for investigating most prokaryote microorganisms are different in many respects from those used for studying one well-known group of prokaryotes, the cyanobacteria, e.g., size, shape, cell structure, and differentiation. Moreover, the organic chemical signals (different organic macromolecules associated with the sheath and membranes) are different. The criteria we use also include features related to the interrelationship between the microorganisms and their immediate environment (see also Westall, 1999; Westall et al., 2000).

Structural characteristics. The structural characteristics concern the organisms as physical entities as individuals as well as their colonies, biofilms, or mats. They include the following: (1) morphological phenomena such as size, shape, evidence for life and death; for example, as in cell division (i.e., evidence for a living process), cell collapse (i.e., evidence for cell death or lysis; this is the process by which an enzyme, released automatically when a cell dies and breaks down the outer cell envelope so that the internal cytoplasm can escape, thus leading to collapse of the cell. This process leads to variations in the surface texture of the cell, such as wrinkling as opposed to the turgid structures and textures typical of living cells), and flexibility; and (2) colony and biofilm/mat characteristics, such as association with a number of other organisms of the same species, association with different species in the same colony (consortium), association with microbially produced polymer (extracellular polymeric substances, EPS), and formation of physical entities, i.e. as individual cells as well as colonies, biofilms, or mats. We also used statistical analysis to evaluate the size-shape range of individual microstructures within individual colonies and for a comparison of different colonies forming in different layers (microenvironments) of the sediment. In this exercise, ~2000 individual structures were measured (diameter and length/width ratios with standard deviation [SD] values) from 20 different colonies in Layers 3, 4, 5, and 6 to obtain the modal diameters of the cells.

Biogeochemical characteristics. The biogeochemical characteristics concern the metabolism of the organisms, such as (1) an organic carbon composition (including the degradation products of specific molecules, in the case of fossil microorganisms; *N.B.* in certain conditions such as hot springs, the microbial structure may be fossilized but all trace of organic carbon may have been removed by oxidation, e.g., Cady and Farmer, 1996); (2) association of other important macro- or micronutrients, such as N, P, S, Mg, K, Ca, Na, Fe, Cr, Co, Cu, Mn, Mo, Ni, Si, W, V, and Zn; (3) the metabolic fractionation of the isotopes of elements such as C, S, N, and Fe; and (4) complexation of other elements, such as heavy metals and rare earth elements (REEs) to organic matter.

Other characteristics related to the metabolic activity of microorganisms can be used as indications of biogenicity, such as biocorrosion. A recent study found corrosion pits in the glassy rinds of early Archean pillow basalts from Barberton, South Africa, that were attributed to microbial activity (Furnes et al., 2005).

Microbe-environment interactions. Microorganisms are surface specific and generally need a substrate for reproduction (except when they are in the planktonic form). An understanding of the interactions between individual microorganisms, their colonies, biofilms, and mats and their microenvironment is therefore very important. This means that study of the fossil microorganisms should go hand-in-hand with study of their immediate microenvironment (hence the multidisciplinary approach that we have used). The information thus obtained provides important clues to potential sources of energy, carbon,

and nutrients. Study of direct interactions of the microbes with their substrates provides information on substrate corrosion, biofilm/mat formation, and sediment stabilization including fossilization. As noted above, the potential rapidity of the fossilization process (in hours to days, depending on the species availability of fossilizing cations and physical environmental conditions; Westall et al., 1995; Westall, 1997; Toporski et al., 2002; Orange, 2004) means that even extremely ephemeral microbial developments have the potential of being preserved. Thus, fossilized microbial communities also contribute to sediment stabilization and, in the case of the early Archean sediments, to their early silicification.

RESULTS

Sedimentology and Mineralogy

The studied sample (Fig. 2) is a chert, composed presently of ~80–99 vol% of cryptocrystalline quartz. The rock texture is layered and shows characteristic features, such as microripples and flaser-linsen bedding, which are typical for sediments deposited in an aqueous, near-shore environment. On the basis of microscopic investigations, these sediments can be classified as volcanoclastic in origin.

The sample consists of a number of micrometer- to millimeter-thick layers, the colors of which alternate between light gray and dark gray. The light gray layers consist of coarser material, rich in large pseudomorphosed volcanic mineral particles (Ti-bearing mica, K-feldspar, amphiboles, glass shards, and mineral debris), glassy precursors, and a higher abundance of well-formed, detrital zircon, secondary monazite, and fluorencite. The volcanic clasts have sizes ranging from 30 to 500 μm. The darker gray, fine-grained material contains almost no large clasts and is formed of intergrown microcrystalline quartz and hydromuscovite. The individual layers of this sample have been numbered for ease of description (Figs. 2C–2E). Each of the layers is traceable laterally on a scale of meters. Further mineralogical details are given in Rouchon et al. (2004a, 2004b, 2005) and Orberger et al. (this volume).

Layer 1 (light colored) consists of flat-lying to slightly channel-bedded (on a centimeter scale) laminae, containing fine-grained (30–100 μm) angular volcanic clasts.

Layer 2 is light colored in hand specimen but in thin section consists of a dense concentration of brownish, very fine-grained clasts outlined by microcrystallites (1–2 μm) of Ti-oxide. Its brownish color is given by the large amount of hydromuscovite pseudomorphs replacing primary volcanic clasts.

Layer 3 is light colored and translucent and consists of two sublayers. The lower part has a speckled appearance in hand specimen due to concentrations of Ti-oxide crystallites (Figs. 2E and 3A–3C). It consists of a 2-mm-thick accumulation of ghost structures having subhedral to euhedral shapes. These structures, now consisting of microcrystalline quartz, range in size from 200 to 500 μm. The microprobe data indicate that the ghost particles represent hydromuscovite replacing K-feldspars and volcanic glass shards. Micrometer-sized Ti-oxide crystals outline the protominerals or protoglass shards, indicating that Ti was liberated during silification of, probably, proto-biotite. Scarce, well-formed crystals of monazite are also present. In texture, this sublayer is well sorted and matrix supported (Figs. 3A and 3B). It is overlain abruptly by a fine, crinkly laminated, millimeter-thin layer of chalcedonic quartz (Fig. 2E). The laminations parallel to the top and bottom of this layer indicate that the quartz precipitated in an open crack.

Layer 4 consists of a 1–2 cm layer of poorly sorted (10–300 μm sized), densely packed, and almost grain-supported, angular volcanic shards (Fig. 3D) exhibiting rippled, flaser-linsen bedding (Figs. 2A and 2C). Ti-oxides invariably outline pseudomorphs of hydromuscovite after volcanic clasts. The finer layers comprising the linsen bedding consist of very fine, clay-sized material.

The bedding laminae on top of Layer 4 appear to be truncated by an overlying, 1-mm-thick, light-colored (in hand specimen) layer (Layer 5) (Figs. 2C–2D and 3E–3F). Although it has the same sedimentological characteristics as Layer 4 in terms of grain size, composition, and sorting, this layer has a cloudy, brownish appearance in optical microscopy (Fig. 3E). The ghost particles are still coated by Ti-oxides, but their outlines are diffuse and the whole layer is richer in Ti-oxide crystallites than the underlying layer. There is a sharp contact between the top of Layer 5 and the base of Layer 6 (Figs. 2D and 3E–3G).

Partially embedded in Layer 5 are large (up to 0.5 cm), irregularly shaped fragments of angular to subrounded, scoriaceous particles (Figs. 2B–2D). The electron microprobe analyses suggest a composition similar to that of the silicified, hydromuscovite-replaced volcanic clasts in Layer 4. Many of these large volcanic fragments exhibit distinct optical and compositional differences between the lower portion embedded in Layer 5 and the upper portion protruding into the overlying Layer 6 (Fig. 2D) that is laterally contiguous with the sharp boundary between Layers 5 and 6. The lower halves of the fragments are heterogeneous in color (brownish gray in thin section but white in hand specimen) and texture. The upper halves often have a translucent, yellow-brown color (compared to the matte, white color of the lower part). In some cases, there is a significant concentration of Ti-oxide crystals at the boundary between the upper and lower parts of these large volcanic fragments. Ti-oxide crystallites also outline the edges of primary structures that we interpret to be quartz-filled vesicles, according to their larger quartz grain sizes and SiO_2 enrichment compared to the groundmass of the fragments. Individual pseudomorphs after volcanic minerals, together with the presence of vesicles, indicate that these fragments may have been pumice. In hand specimen, a millimeter-thick, whitish (in hand specimen) surface continuously coats the top of Layer 5 and the pumice fragments (Fig. 2D). Stylolites are sometimes formed below and/or around the pumice fragments and along bedding-parallel planes within Layer 5, especially closer to the intruding chert vein.

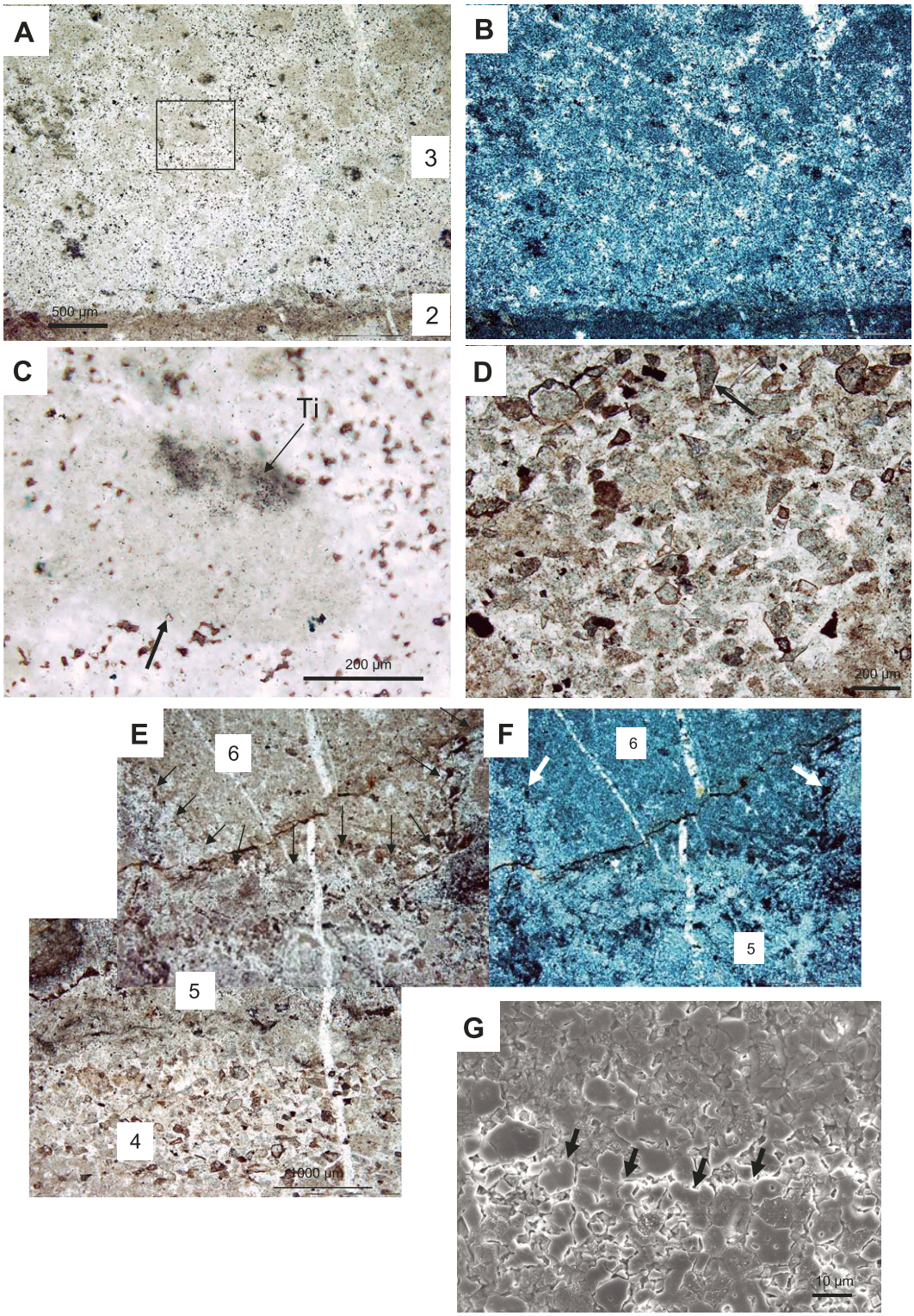

Figure 3. Thin section photomicrographs. (A, B) Normal light and polarized light images of highly silicified, ghost volcanic particles in Layer 3. Layers shown marked by numbers. Box marks location of (C). (C) Detail of one of the ghost particles (lower edge marked by an arrow) with a concentration of minute Ti oxide crystallites (Ti) at its upper edge. (D). Detail of the angular volcanic detrital particles whose sharp outlines (e.g., arrow) are caused by presence of Ti oxide crystallites on their surfaces (cf. Orberger et al., this volume). (E, F) Top of Layer 4, Layer 5, and base of Layer 6. Layer 5 is compositionally and texturally the same as Layer 4, but in thin section appears more diffuse. The top of Layer 5 is shown by black arrows (E), whereas the edges of two pumice fragments are indicated by white arrows (F). (G) SEM photomicrograph of a delicately HF-etched, cut surface showing clear boundary between Layers 5 and 6 (arrows).

Layer 6 is dark in hand specimen and ranges in thickness between 1 and 2 cm along strike (Fig. 2D). It is very fine grained and homogeneous, containing rare, small (20–100 μm) ghost particles (Figs. 2D and 3E–3F). It has a similar composition to that of the underlying volcanic layers, suggesting that it probably consisted of a volcanic dust protolith replaced by very fine-grained quartz (hence the black color in hand specimen) and hydromuscovite. The lower part of this layer is characterized by a fine, brownish horizon (in optical microscopy) that conformably follows the top of Layer 5, including the pumice fragments (Fig. 12A). Blocky, carbonaceous particles with a subrounded shape and sizes ranging from 6 to 20 μm occur in Layers 5 and 6 (Fig. 4). In terms of texture and structure, these particles can be divided into two groups. One type has a rather homogeneous, granular texture and a composition that includes traces of S and Cl, as well as SiO_2. The other type has a filamentous texture and has filaments similar to those described below (in the Microfossils section) attached to it. Sulfur and Cl do not appear in the EDX spectra of this type of carbonaceous clast (Fig. 4C).

Layer 7 is light colored and consists of flat-lying laminae of relatively coarser (50–300 μm), volcanic particles (Fig. 2C). The grains in the lowermost horizon of Layer 7 have been pressed into the underlying sediments in a texture suggesting

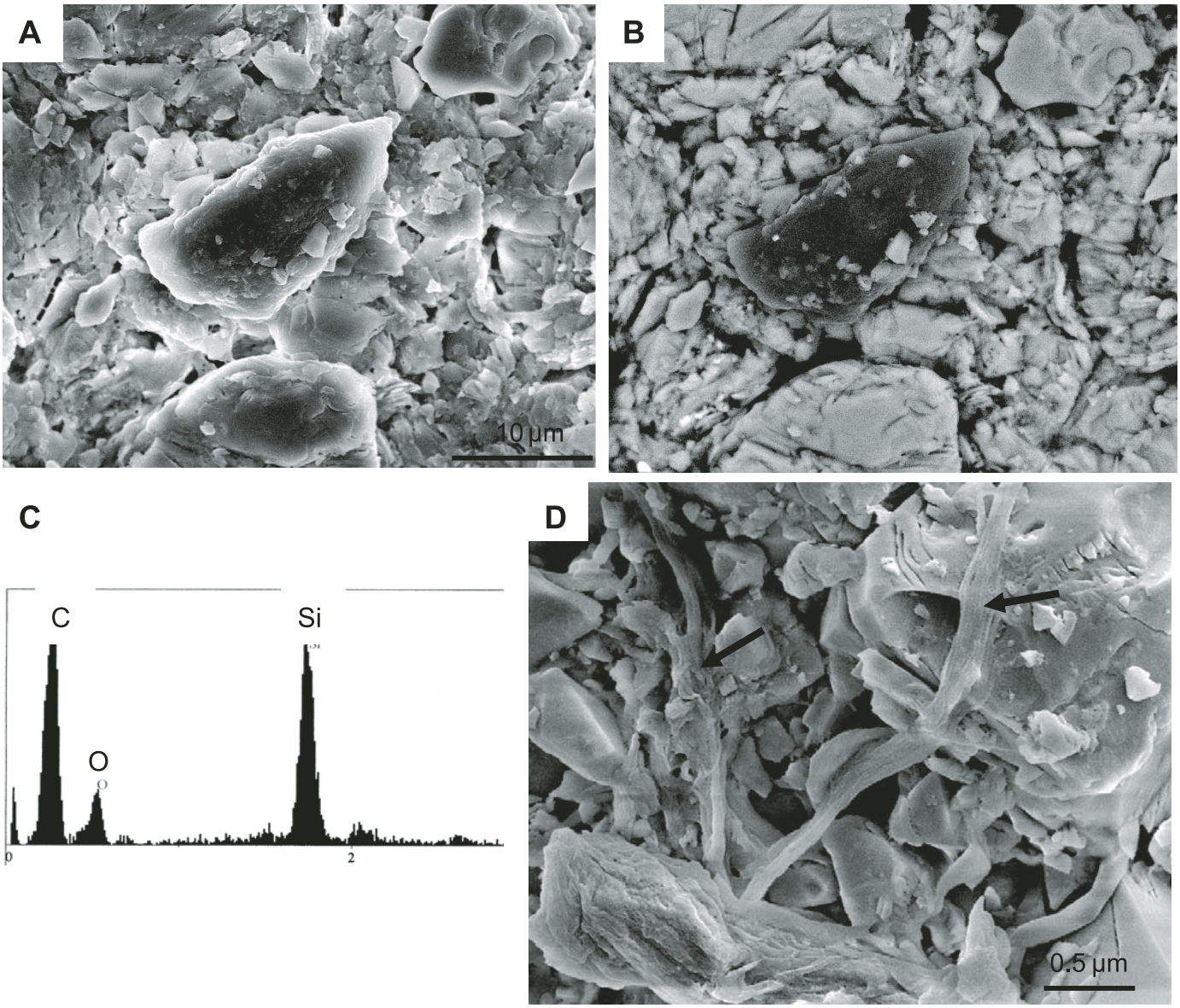

Figure 4. (A, B) SEM photomicrographs in secondary (A) and backscattered (B) electron mode of a subangular, detrital, carbonaceous particle in Layer 4. (C) EDX (electron diffraction X-ray spectrometry) spectrum of the large carbonaceous particle in the center of (A). (D) Detrital, fibrous, carbonaceous particle at the base of Layer 6 with degraded, striated filaments (arrows) attached to it that are similar to those in Figure 7.

millimeter-scale soft sediment deformation. The lowermost part of this layer is grain-supported, but the texture becomes matrix-supported in the midlayer. Clast sizes increase toward the top, which is marked by 1 mm-sized, angular fragments of euhedral protominerals having heterogeneous compositions and partially resembling the pumice fragments at the top of Layer 5. Layer 7 is overlain by another dark layer of microcrystalline quartz, replacing fine volcanic dust (a few μm) that constitutes Layer 8 (resembling Layer 6). It, in turn, is overlain by light-colored, flat-laminated, relatively coarser (30–300 μm) material (Layer 9).

The detailed micropaleontological studies were made in Layers 3–6.

Geochemistry

Orberger et al. (this volume) note that although the geochemical compositions of the light and dark-colored layers in this chert are similar, there are some differences as a result of the higher concentration of hydromuscovite (replacing protominerals, such as Ti-bearing mica, K-feldspar, amphiboles, glass shards, and higher contents of accessory minerals, monazite, and zircons) in the light-colored layers. Vanadium (associated with the Ti-oxides), Sr, and Rb (associated with hydromuscovite) are enriched in the light layers, as are Zr, Y, W, Nb, Ta, Ba, and HREE (heavy rare earth elements). LREE (light rare earth element) compositions of both dark and light layers are the same.

Bulk carbon contents for individual layers in this rock are generally low, 0.01%–0.05%, but nuclear microprobe spot measurements made on different volcanoclastic protominerals show wide variations from 0.007 to 0.859 atomic % in all the layers, irrespective of their grain size (Rouchon et al., 2004a, 2004b, 2005). Nitrogen contents measured on the same particles were also variable (0.013–0.125 at %), as were C/N ratios (0.08–20.95). Rouchon et al. (2004a, 2004b, 2005) found that there was no correlation in distribution between the N and the C, apart from their common association with hydromuscovite pseudomorphs. It is likely that the N occurs as NH_4^+ in the K^+ lattice sites of the hydromuscovite, and the C occurs dispersed as an organic phase or possibly as HCO_3^- in the (OH^-) site of the hydromuscovite structure. The SEM observations confirm the presence of an organic carbon component associated with the hydromuscovite (see below).

Carbon and Nitrogen Isotope Analyses by Stepped Combustion

The stepped combustion studies show that, for all the samples analyzed, there is a low temperature peak of carbon release at temperatures between 200 °C and 600 °C, with a maximum at 300–400 °C (Fig. 5). In the crushed samples this peak represents the main carbon release. At higher temperatures, the amount of C released is much smaller, and there is a gradual increase of carbon yield with increasing temperature. The uncrushed sample shows, however, a different release pattern (Fig. 5F): most of the carbon is released at high temperature with a peak at 1100 °C. Carbon content shows a positive correlation with sample weight (Fig. 5G). Note that although the measured amounts are positively correlated with the sample weight, the concentrations, in contrast, are negatively correlated. This can be explained mathematically, as follows. Amounts of the intrinsic carbon (C_{int}) are proportional to the sample weight (P). Amounts of the contamination carbon (C_{cont}) are proportional to the sample surface area or $P^{2/3}$. The total concentration ($C_{int}+C_{org}$)/P is proportional to ($P+P^{2/3}$)/P or $1+P^{-1/2}$, as illustrated in Figure 5G.

In general, the isotopic compositions of the carbon released at low temperatures and at high temperatures are similar and range from –22‰ to –30‰ (Figs. 5A–5F). The bulk compositions range from –25.9‰ to –27.8‰ (Table 1).

Raman and High-Resolution TEM Investigations of the Kerogen

The TEM micrographs of Figure 6A show that the carbonaceous matter consists of small (nanometer-sized), more or less parallel-oriented, polyaromatic layers that are typical for mature kerogen (cf. Boulmier et al., 1982; Oberlin, 1989). The Raman spectrum (Fig. 6B) consists of two peaks at 1346 nm (D1 defect band) and 1586 nm ($E_{2\,g}$ band); the ratio D1/G indicates moderately mature kerogen (Beyssac et al., 2002a, 2002b),found in Layers 3–6.

Microfossils

In Layers 3, 4, 5, and 6 we have identified a number of microstructures that we interpret as representing fossil microorganisms and colonies or biofilms thereof. They include: (1) filaments with a modal diameter of 0.3 μm and lengths of up to more than 40 μm (they are never observed in their entirety); (2) coccoidal structures having two modal sizes of 0.45–0.5 μm and 0.75–0.8 μm; (3) rod-shaped structures ~0.8 μm in length and 0.4 μm in width; and (4) a film-like substance that embeds the other microstructures, as well as coating and sometimes completely embedding underlying sediment particles. We interpret these structures as fossilized filamentous, coccoidal, and rod-shaped microorganisms, respectively, and the film as extracellular polymeric substances (EPS) (see Discussion, below). Associations of these structures are interpreted as colonies or biofilms. These observations are summarized for each layer in Table 2.

Filaments

The best-preserved filaments retain a cylindrical form throughout their length and have diameters ranging from 0.3 to 0.45 μm (Fig. 7). The filaments are striated lengthwise (Figs. 7A and 7C), a feature that may be related to a fundamental characteristic of the outer cell wall of a particular species (a similar

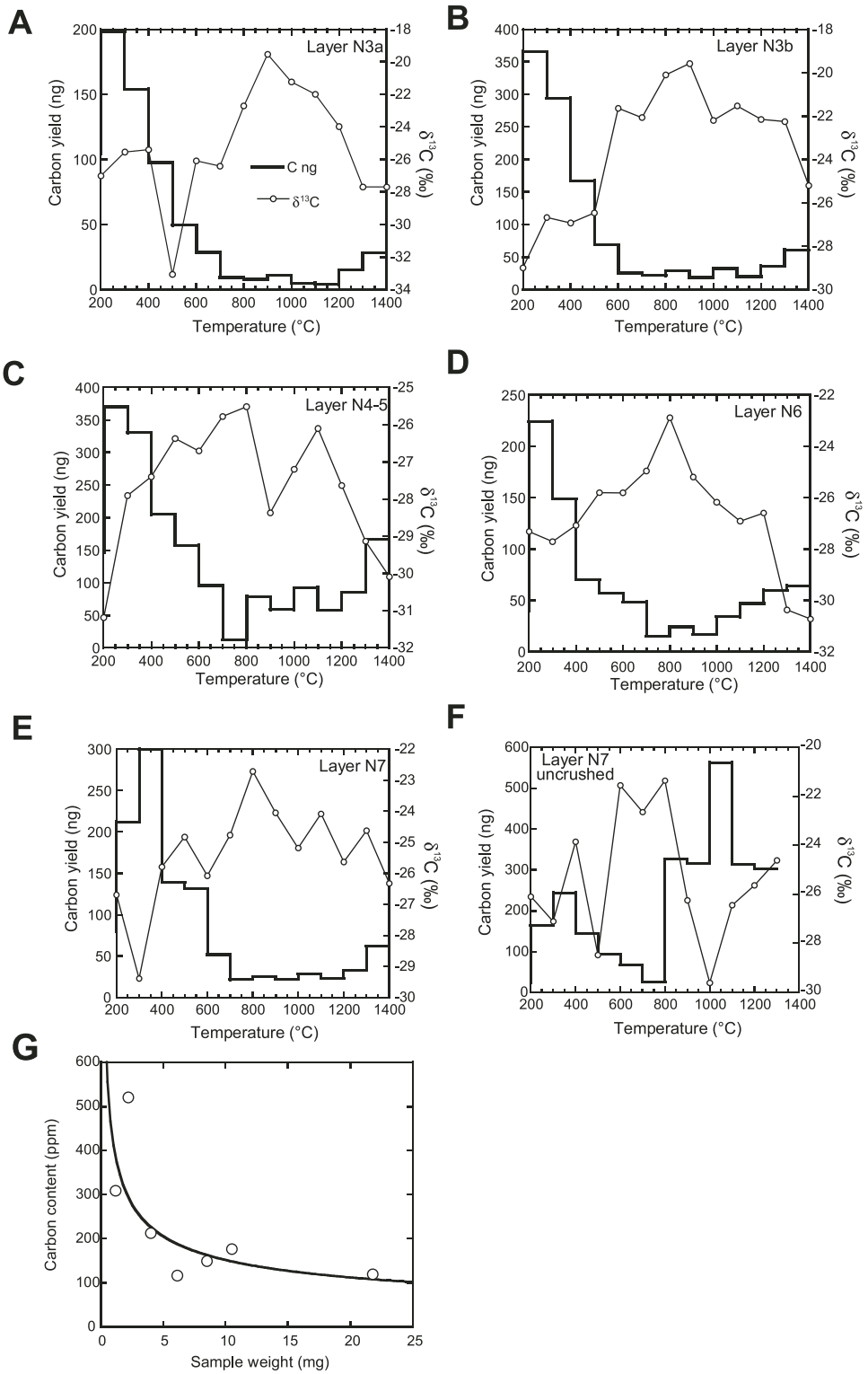

Figure 5. (A–F) Carbon content and isotopic compositions from the stepped combustion analyses of Layers 3–7. (A–E) are the results from crushed samples: (A) lower part of Layer 3; (B) upper part of Layer 3; (C) Layers 4+5; (D) Layer 6; (E) Layer 7. (F) Results for the uncrushed sample of Layer 7. (G) Carbon content as a function of sample weight. [*N.B.* although the measured amounts are positively correlated with the sample weight, the concentrations, in contrast, are negatively correlated. This can be explained mathematically. Amounts of the intrinsic carbon (Cint) are proportional to the sample weight (P). Amounts of the intrinsic carbon (C_{int}) are proportional to the sample weight (P). Amounts of the contamination carbon (C_{cont}) are proportional to the sample surface area or $P^{2/3}$. The total concentration (C_{int}+C_{org})/P is proportional to ($P+P^{2/3}$)/P or $1+P^{-1/2}$].

TABLE 1. BULK DATA FOR THE CARBON CONTENT AND CARBON ISOTOPE ANALYSES OF LAYERS 3 TO 7

Layer N	Weight (mg)	Concentration (ppm)	$\delta^{13}C$ (%)
3a	6.11	117	–26.8
3b	8.50	150	–25.9
3b	1.17	309	–
4–5	10.50	177	–27.8
6	4.00	213	–27.3
7	21.80	120	–26.1
7	2.18	520	–26.2

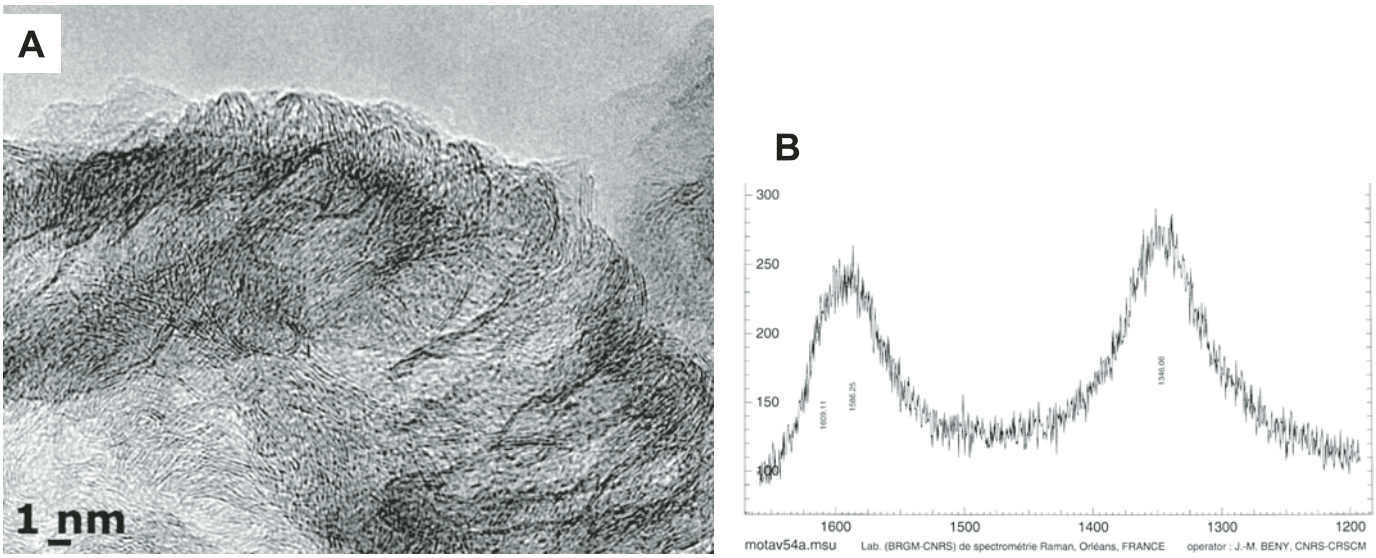

Figure 6. (A, B) High-resolution TEM photomicrograph of carbonaceous material liberated by acid maceration from Layers 5 and 6. The kerogen is characterized by small packets of short, more or less parallel-oriented polyaromatic layers, indicating some crystallographic ordering, although still far from the graphite stage. Such a structure is similar to that found in mature kerogens from biological precursors found in rock-parent of oil (Boulmier et al., 1982). (B) The ordering of the kerogen is confirmed by Raman spectroscopy that shows both the graphite peak at 1586 as well as the amorphous peak of carbon at 1346.

TABLE 2. SUMMARY OF THE MICROFOSSIL CHARACTERISTICS FOR EACH LAYER OF THE KITTY'S GAP CHERT STUDIED

Sediment layer	Filaments diam. µm range mode	Comment	Coccoids			Comment	Rods	Colonies/biofilm	EPS
			diam. µm		SD				
			Range	Mode					
6 (dark) midlayer		Rare (1)	(1) 0.35–0.65	0.5	0.1	Relatively	None	"Carpet" colonies	Yes
			(2) 0.7–0.8	0.77	0.05	well preserved		>100s individuals 20–30 µm	
6 (dark) basal layer	0.26–0.7 0.35	Common striated surfaces, poor preservation	(1) 0.35–0.65	0.4–0.5	0.06–0.07	Poorly preserved dispersed groups	Rare (2) 0.8 × 0.4 µm	Biofilm of filaments, coccoids, rare rods, EPS "glued" particles	Copious smooth
			(2) 0.7–0.8	0.75	0.06–0.07	Chains <10 cells dislocated cells			
5 (light)	0.2–0.5 0.35	Relatively common striated surfaces variable preservation	(1) 0.35–0.65	0.4–0.43	0.04–0.07	Moderately preserved dispersed groups	None	Loose biofilm of filaments coccoids, EPS, "glued" particles	Smooth to granular
			(2) 0.7–0.8	0.75	0.04	Chains dislocated cells			
4 (light)	None		(1) 0.35–0.65	0.4–0.5	0.05–0.14	Moderately preserved dispersed groups		Loose colonies	Yes
			(2) 0.7–0.8	0.73	0–0.08	chains dislocated cells			
3 (translucent)	0.1 (1 filam.)	Badly degraded fragment	(1) 0.35–0.65	0.44–0.51	0.04–0.1	Moderately preserved dispersed groups	Rare (2) 0.8 × 0.4 µm	"carpet" colonies >100s individuals 20–30 µm	Yes
			(2) 0.7–0.8	0.68–0.87	0.05–0.08	chains dislocated cells			

Note: SD—refers to Standard Deviation; EPS—refers to Extracellular Polymeric Substances.

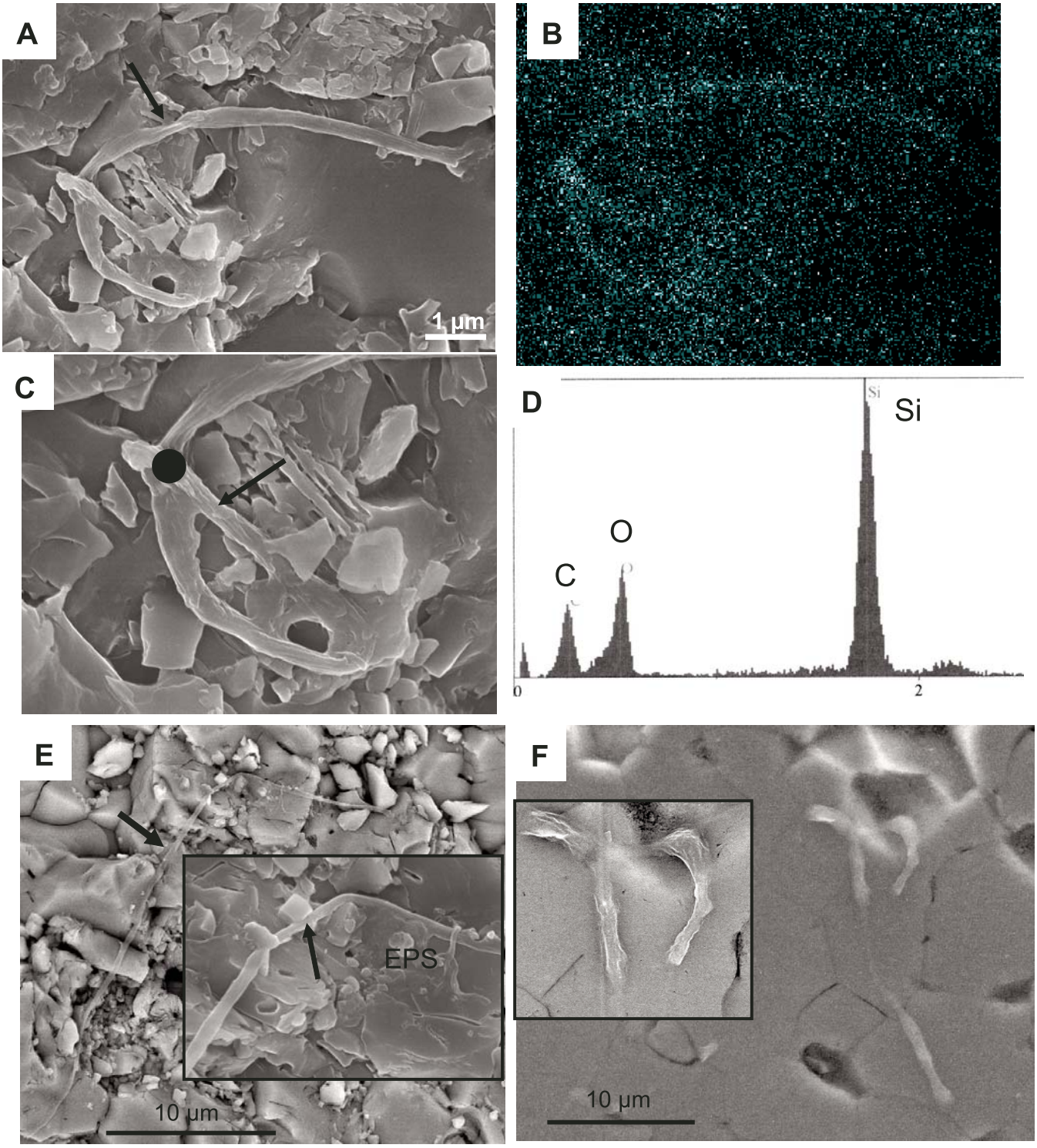

Figure 7. Filamentous microfossils from top of Layer 5. (A) Secondary electron photomicrograph of a fragment of a filament (note collapsed section of tubular structure—arrow). (B) Carbon map of same structure. (C) Detail of filament showing length-parallel striations (arrow). (D) EDX (electron diffraction X-ray spectrometry) spot analysis of filament (analysis made at black spot in [C]). (E) Detail of a long portion (>30 µm) of a filament (arrow) that has retained its tubular shape for its entire length. (Inset) Secondary electron photomicrograph detail of the striated filament. Note (i) adjacent small rectangular particle that apparently grew contemporaneously with the filament and (ii) EPS (extracellular polymeric substances) associated with filament. (F) Secondary electron photomicrograph of filaments cutting across boundaries of quartz grains in a lightly etched thin-section surface. (Inset) Detail of collapsed appearance of filaments.

phenomenon has been observed on filamentous bacteria from a hot spring environment, S. Cady, 2002, personal commun.) and/or to the degradation and shrinkage process after cell death. As a result of this characteristic, highly degraded filaments appear as frayed, fibrous strands, some of which may only be 0.1 μm in diameter (Fig. 8). All the filaments present a sinuous morphology. EDX spot measurements (Fig. 7D) document C, O, and Si, whereas carbon mapping shows that they are distinctly carbonaceous (Fig. 7B). The filaments are associated with patches of polymer and very often with coccoidal structures exhibiting features attributed to cellular division (see below) (Fig. 8). Filaments were observed in the surface of the slightly etched thin section, where they are completely embedded in quartz crystals (Fig. 7F). Filaments are common at the base of Layer 6 and relatively common at the top of Layer 5. Rare fragments of filament occur in Layers 3 and the main part of Layer 6.

Coccoidal Structures

Coccoidal structures are numerous in all layers but occur in different types of associations (colonies) in different layers (Table 2). The size/shape statistical analyses of >2000 individuals from 20 colonies showed that the coccoidal structures fall into two main size categories: one group with modal diameters between 0.4 and 0.5 μm (standard deviation [SD] 0.04–0.1) and the second with modal diameters mainly between 0.73 and 0.77 μm (SD 0–0.07) (Figs. 9A, 9C, and 10D). Most of the coccoids are surrounded by a halo of EPS (Figs. 9B, 9C, and 10A). Many of them are attached to each other either by compromised boundaries or by a neck of EPS, as if in cell division (Figs. 9 and 10). Occasionally the two parts of the compromised cells exhibit lateral dislocation, where one of the attached cells is turgid in shape but the other cell is deflated and presents an irregular surface texture (Fig. 10D). Deflation of the coccoids produces a rough, wrinkled outer surface texture, indicating that the structures were hollow (Figs. 10A, 10D, and 10E).

The coccoids occur in colonies of varying numbers of individuals. Loose associations consist of groups of a few coccoids (five to some tens) embedded in EPS that are irregularly dispersed on the substrate but occur within distances of a few μm from each other. Frequently, the coccoids in the loose colonies may form chains consisting of 3 to, at most, up to 10 individuals (Figs. 10A, 10C, and 10E). The most spectacular coccoidal colonies consist of dense associations numbering many hundreds of individuals, all embedded in EPS. We term them "carpet" colonies (Figs. 9A and 11). Such colonies have irregular but relatively distinct outlines and may be some tens of μm in size. EDX spot analyses and carbon mapping clearly demonstrate the carbonaceous nature of the coccoids and the colonies they form (Fig. 11). Layer 3 and the main part of Layer 6 (but not its base) contain exclusively "carpet" colonies. The looser colonies occur in Layers 4 and 5 as well as at the base of Layer 6, where, with the exception of Layer 4, they are commonly associated with the filaments described above (Figs. 8 and 10C).

Although the distribution of the loose and "carpet" colonies of coccoidal structures is heterogeneous within each particular layer, they are clearly concentrated around the edges of the hydromuscovite-replaced volcanic protoliths (Fig. 11C).

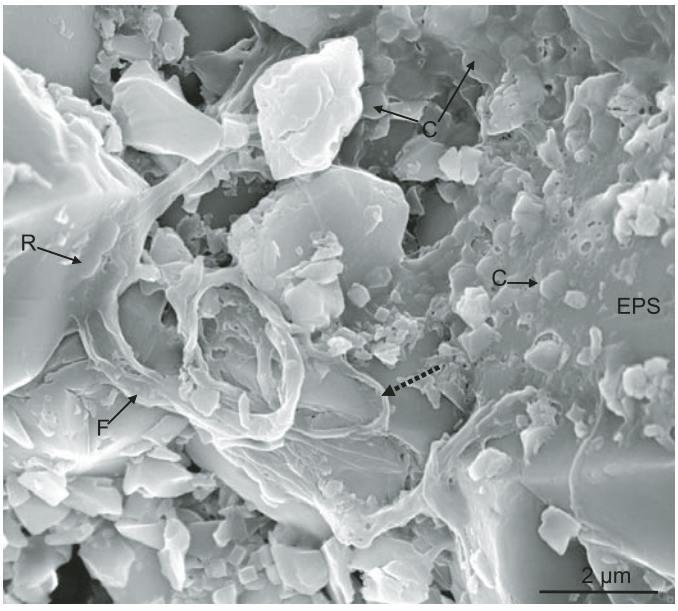

Figure 8. Secondary electron photomicrograph of the biofilm formed at the base of Layer 6. It consists of filaments (F), coccoids (C), rod-shaped microorganisms (R), and EPS (extracellular polymeric substances). The filaments are highly degraded, having broken down into fine strands in places (dotted arrow). The rod-shaped microorganisms show cell division, as do most of the coccoids. The EPS appears as a thin film that coats the sediment particles and is locally perforated by holes.

Rod-Shaped Structures

Rod-shaped structures ~0.4 μm in width and 0.8 μm in length occur rarely in this volcanoclastic sediment (Figs. 8 and 10F). Isolated individuals were observed in close association with coccoids in Layers 3, 5, and 6. The coccoid-filament association at the base of Layer 6 contains one example of two rods attached to each other by a compromised boundary at their extremity (Fig. 10F). EDX spot measurements document relatively high concentrations of C associated with the rods.

Exopolymeric Substances (EPS)

EPS occurs in two modes: (1) as an intimate extension of the coccoidal microstructures, coating them like a halo and linking dividing cells (Figs. 9B, 9C, 10A, 10C, and 10E), and (2) as a laterally extensive material that coats or embeds the microbial colonies (Figs. 8, 9A, and 11) and the surrounding mineral particles (Figs. 8 and 12B–12F). The laterally extensive EPS may have a smooth (Fig. 8) or a granular surface (Figs. 12E and 12F), which often exhibits holes and/or a cracked texture (Figs. 8, 9A, and 10A). EPS is ubiquitous throughout the layers.

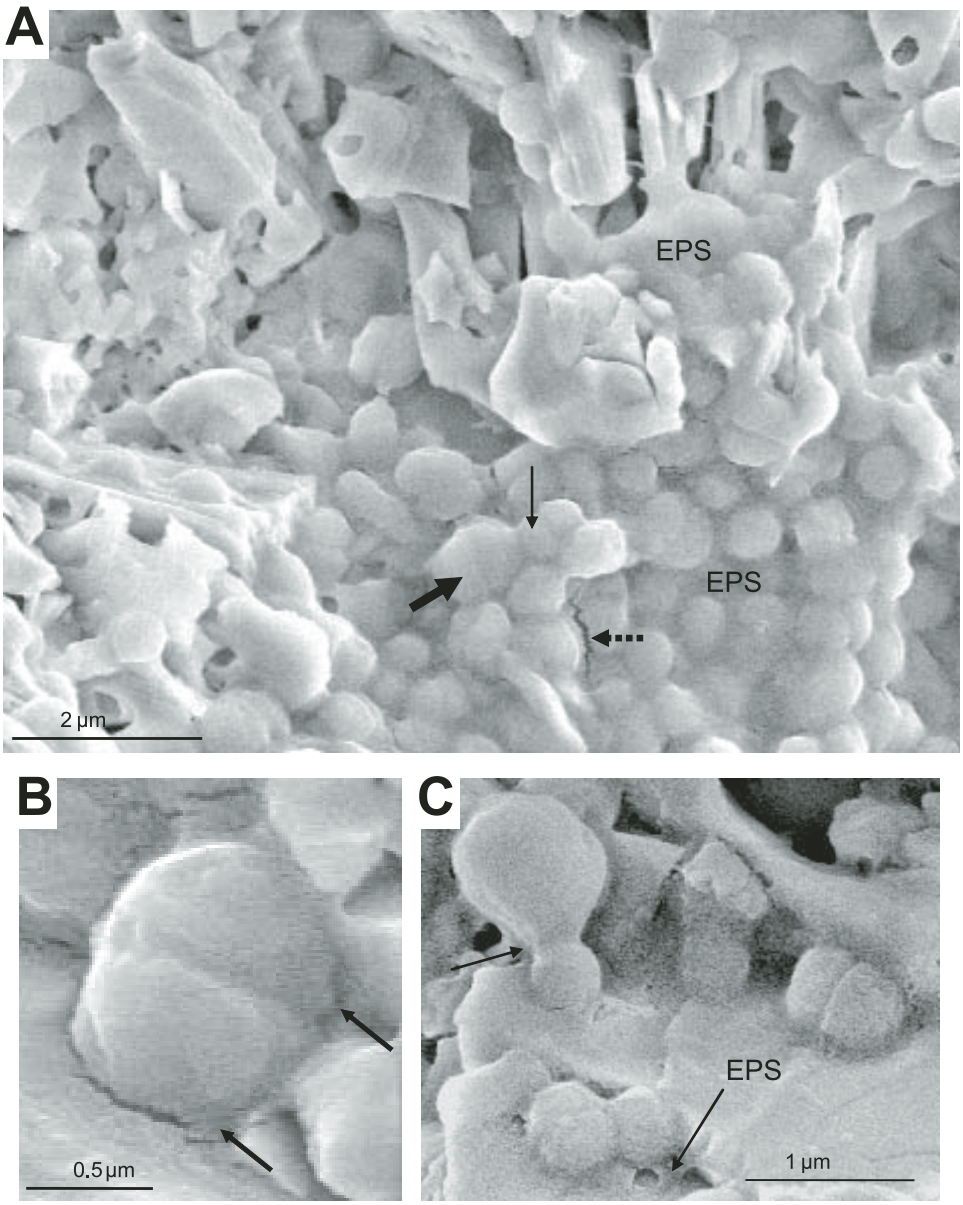

Figure 9. Secondary electron photomicrograph of coccoidal microfossils. (A) Part of a "carpet" colony of coccoids (Layer 3) at edge of a large, silicified, hydromuscovite-replaced, volcanic particle (see Fig. 11A). The hydromuscovite is visible as foliated minerals at the top of the micrograph. Note the EPS (extracellular polymeric substances) coating both the minerals and the coccoids. Two species of coccoids having two distinct modal sizes coexist in this colony: larger coccoids (large arrow) have a modal size of 0.75 µm, whereas smaller ones are 0.45 µm (small arrow). The dotted arrow points to a desiccation crack in the EPS. (B) Detail of a dividing coccoid from Layer 5. Initial separation of two parts of dividing cell, typical of cell division by fission, is clearly visible. Note collapsed, cell-bound EPS around edge of microorganisms (arrows). (C) Two species of dividing coccoids having different modal sizes from Layer 4. Note cell-bound EPS surrounding cells.

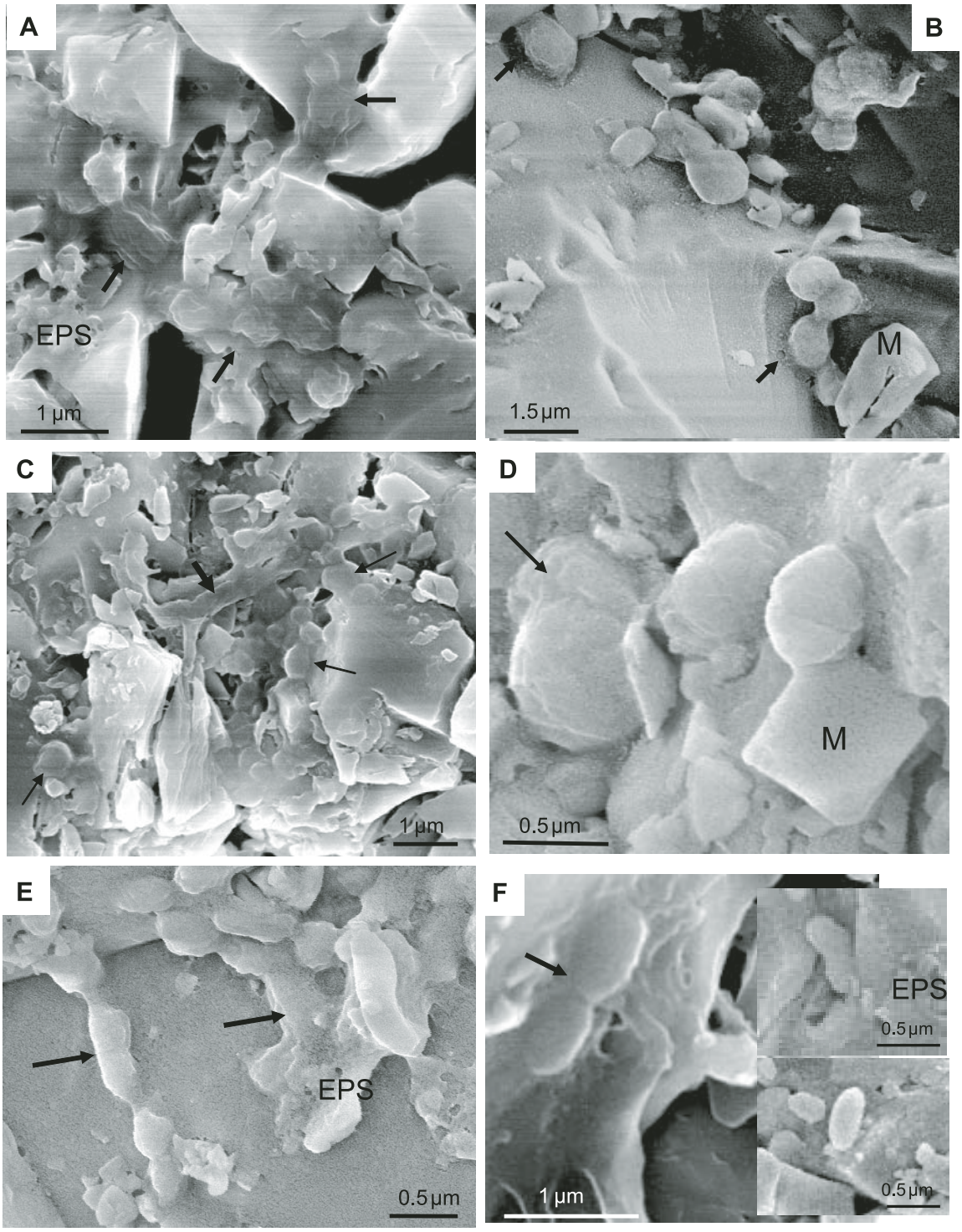

Figure 10. Secondary electron photomicrographs of coccoidal and rod-shaped microfossils in Layers 4, 5, and 6. (A) Chains of collapsed and deflated coccoids, coated in cell-bound EPS (extracellular polymeric substances; arrows) from the base of Layer 6. Note wrinkled texture on surface of these fossilized microorganisms, indicating they were dead (cell collapse and lysis) before fossilization. (B) Dividing coccoids with cell-bound EPS from base of Layer 6. M—mineral fragment. (C) Consortium consisting of a degraded filament (thick arrow) and many coccoids (thin arrows) from top of Layer 5. (D) Coccoids of two sizes in cell division in a pumice fragment. Note that one of larger coccoids has collapsed (indicating cell death) while other half still exhibits a vital turgid aspect. The mineral (M) obviously grew in coexistence with coccoids, since it appears to be attached to a small, dividing coccoid. (E) Highly degraded coccoid chains (arrows) from the base of Layer 6. (F) Rod-shaped organisms (*N.B.* structures resembling rod-shaped microorganisms are very rare in these sediments). Main micrograph shows a dividing rod from biofilm in Figure 8, the other two occur in Layer 3.

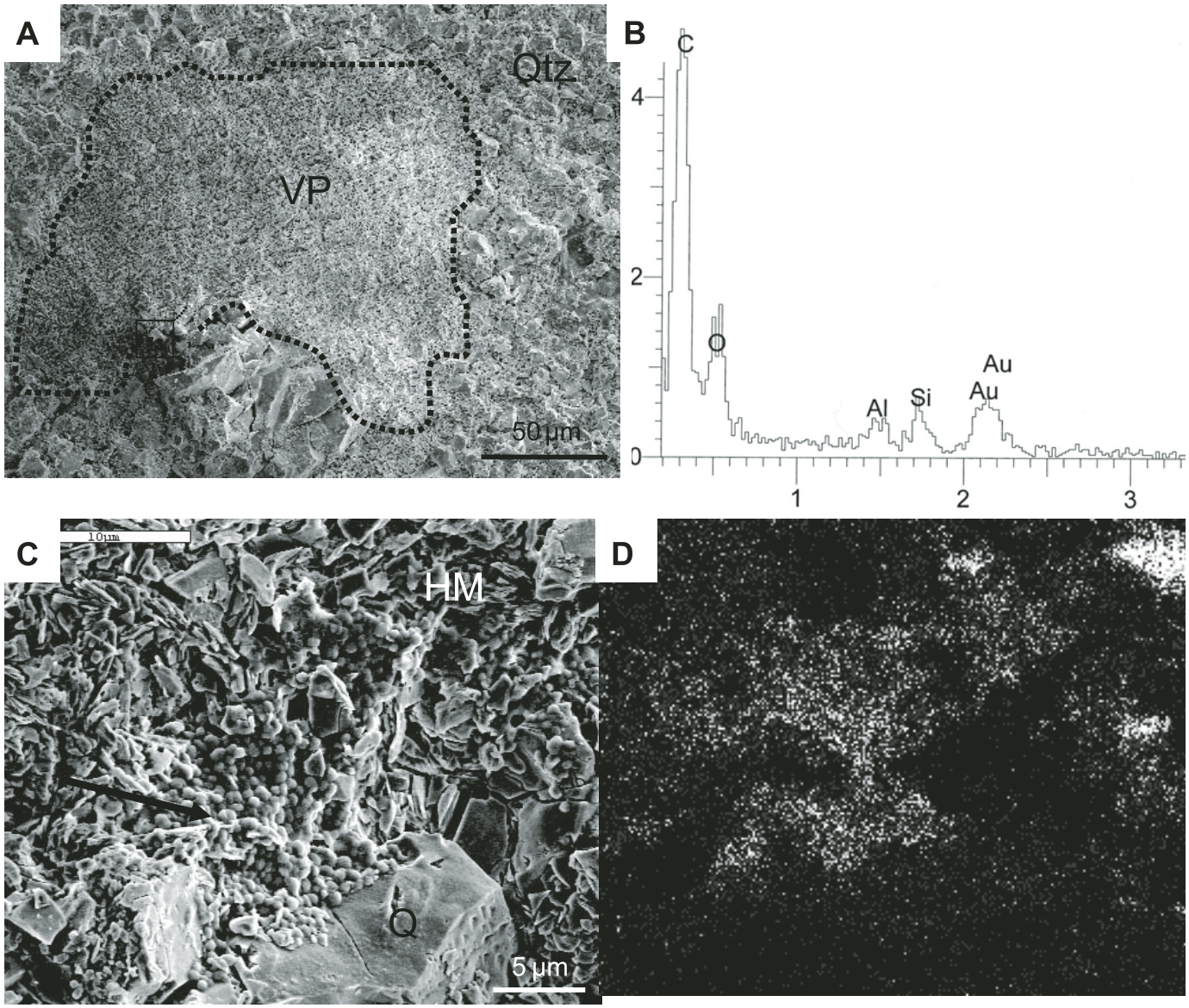

Figure 11. "Carpet" colonies in Layer 3. (A) Low magnification secondary electron photomicrograph of one of the volcanic particles (VP) in Layer 3 (dotted outline) (cf. Figs. 2E and 3A). Numerous "carpet" colonies occur around its edge. Rectangle represents location of "carpet" colony shown in (C) and in Figure 9A. (B) EDX (electron diffraction X-ray spectrometry) spot analysis of center of colony showing strong carbon concentration. (C) Secondary electron photomicrograph of a "carpet" colony (arrow) (see also detail in Fig. 9A) located at edge of hydromuscovite (HM)-replaced volcanic particle and quartz (Q) matrix. (D) EDX carbon map of colony showing that carbon is restricted to colony.

Colonies and Biofilms

As noted above, the filaments, coccoids, and rods occur with other cells of the same morphology and size and sometimes with different types of cells, in associations embedded in EPS that represent microbial colonies (Figs. 8, 9A, 10A, 10C, and 10E). The composition and style (i.e., loose or carpet colony, biofilm) of the colonies in each sediment layer are different. Layer 3 is characterized by coccoidal carpet colonies; loose colonies of small coccoid associations and chains of coccoids occur in Layer 4; at the top of Layer 5 and at the base of Layer 6, a consortium of filaments, coccoids, and (rarely) rods form biofilms; and the main part of Layer 6 consists of coccoid carpet colonies. The biofilm at the base of Layer 6 is moderately well developed and laterally extensive. It is associated with thick quantities of EPS that cement also the sediment particles (Figs. 12B–12F). It coincides with the thin brownish layer, observed in thin section, that conformably coats the top of Layer 5, including the pumice fragments (Fig. 12A). The biofilm in Layer 5 is more diffuse than that at the base of Layer 6.

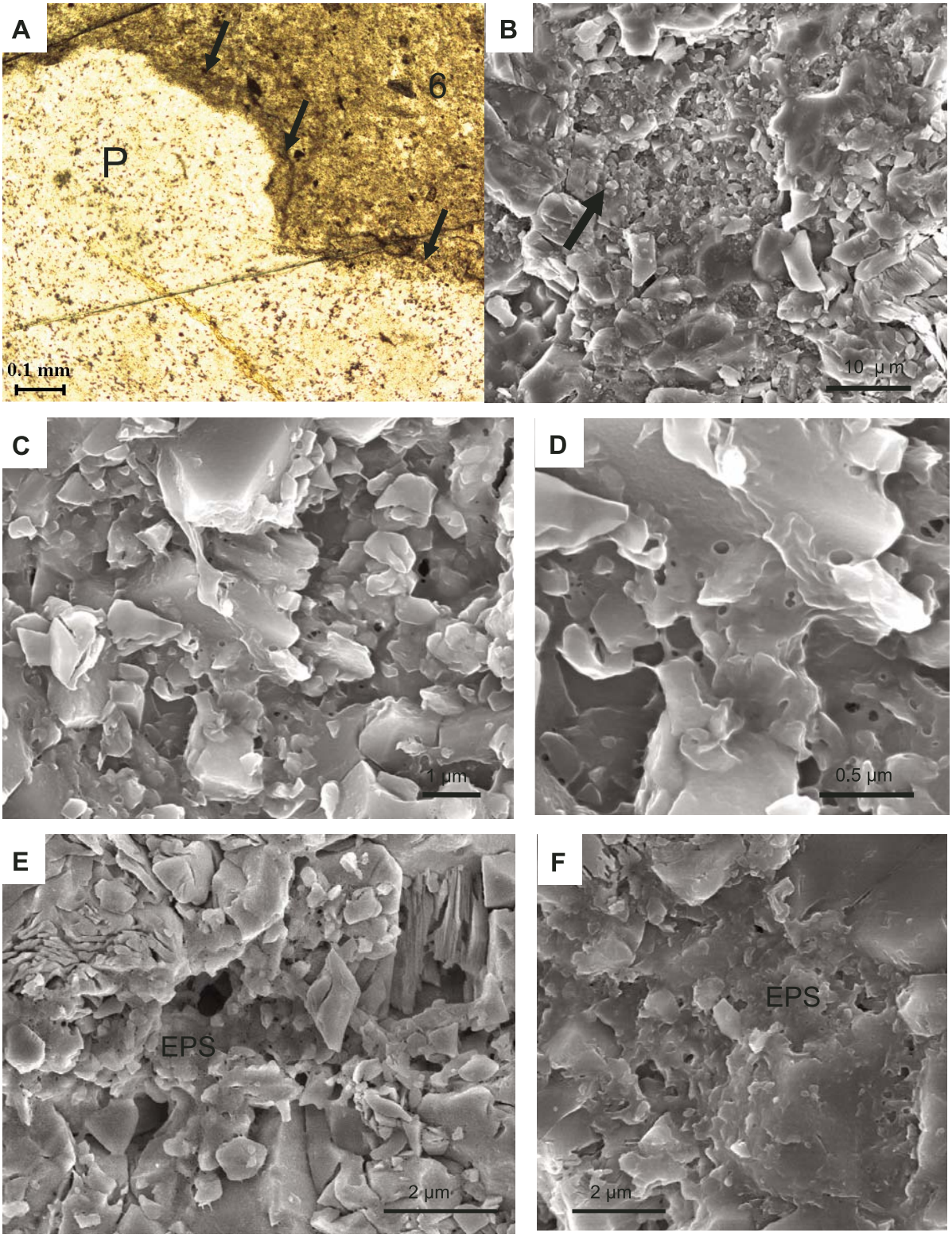

Figure 12. Extracellular polymeric substances (EPS). (A) Thin-section photomicrograph of top of layer 5, including a pumice fragment (P) and base of Layer 6. Note faint brown line at base of Layer 6 (arrows) that is conformable with underlying sediment surface and probably represents a biofilm (cf. Fig. 8). (B–D) Secondary electron photomicrographs of the layer corresponding to the brown line in (A). (B) Small zones of EPS–cemented, cryptocrystalline quartz (arrow) are associated with consortia of microfossils, such as that shown in Figure 8. (C, D) Detail of fine EPS cemented cryptocrystalline quartz particles. Note holes in EPS (D). (E, F) Granular EPS cementing sediment particles together in main part of Layer 6.

DISCUSSION

Sedimentological Environment

de Vries (2004) has demonstrated that the overall sedimentary environment for the "Kitty's Gap Chert" is a channel that was gradually filled up with sediment, termed a channel-and-flat environment. Within this broad environmental context, each layer in the sediment samples that we have studied reflects slightly different and alternating conditions related to different energetic levels of the water transporting the sediment. The light gray layers containing relatively coarse clasts were deposited in a higher energy regime than the dark gray layers consisting of dust-sized material. The source of the sediment must have been local, as the detrital particles, including those of carbonaceous composition, are extremely angular, indicating that they have not been transported far. Moreover, the filamentous carbonaceous particles always have degraded filaments attached to them (Fig. 4D) that are morphologically identical to those formed in situ in the biofilms of Layer 5 and at the base of Layer 6 (see discussion below regarding the endogeneity of the microfossils), suggesting that they formed in a similar, nearby environment.

Layer 3 stands out even in the hand specimen because of its multilayered, translucent appearance (Fig. 2E). It is the most highly silicified of the sedimentary layers studied, and most of the hydromuscovite-replaced volcanic clasts have themselves been almost completely replaced by silica. The fact that it consists of the same protoliths as Layer 2 and that it is separated from Layer 4 by a bedding-parallel chalcedony vein suggests it was subjected to a postdepositional, early diagenetic, secondary silicification event (see section below on the timing of microbial silicification).

The pumice fragments embedded in Layer 5 (Fig. 2D) probably represent ash fall deposits from a distant volcanic eruption. They show a sharp visual and compositional distinction between the translucent, orange-colored, hydromuscovite (with localized quartz replacement) upper part and the opaque, whitish, mainly quartz lower part that corresponds to the level of embedding in the top of Layer 5 (Fig. 2D). The quartz replacement of the lower part of the pumice fragments may indicate a higher saturation in silica in the sediment pore waters. The sharp distinction between the relatively coarse-grained Layer 5 and the very fine-grained Layer 6 clearly represents a significant change in the energy conditions under which the respective layers were deposited, from higher to very low energy conditions.

Biogenic or Abiogenic Origin of the Microstructures

We interpret the filamentous, coccoidal, and rod-shaped structures as microbial filaments, coccoids, and rods, respectively. Their associations are interpreted as microbial colonies, whereas the multispecies associations at the top of Layer 5 and base of Layer 6 are interpreted as microbial biofilms. Our interpretations are based on the following evaluations.

Environmental Habitat

The volcanoclastic sediments deposited in this channel-and-flat environment provided a range of microenvironments that could have hosted life, including the surfaces of the detrital particles (both exposed on the sediment surface and within the seawater-filled pore spaces of the soft sediments), as well as the boundary between Layers 5 and 6 that represents a relatively stable sediment surface.

Morphological Characteristics

The microstructures described above exhibit a range of morphological characteristics that is typical of the individual and colonial aspects of prokaryote microorganisms but not of organisms such as cyanobacteria (Westall, 1999, 2003; Madigan et al., 2000).

Filaments. The size and shape of the filaments are the same as those of modern microorganisms (Madigan et al., 2000; Handley, 2004). Moreover, their sinuosity signifies that they were formed of a material that could be plastically deformed. Partial deflation of their tubular structure suggests that they were hollow when fossilized. This implies that the filaments were already dead and had experienced cell collapse due to lysis and loss of their internal cytoplasm before fossilization. The fragmented nature of most of the filaments also supports this interpretation. The striation along the lengths of the filaments is intriguing: as noted above, similar features have been observed on other microbial filaments in hot spring environments. Although not as common as the coccoidal structures, the filaments are relatively common in Layer 5 and at the base of Layer 6 and occur in association with colonies of coccoidal structures, rare rods, and copious amounts of polymer.

Coccoids. The coccoidal structures are interpreted as being microbial in origin due to the following.

1. The consistency of their size and shape with those of modern coccoidal microorganisms (Madigan et al., 2000) (*N.B.* the two different sizes of coccoids probably represent two different species).

2. The regularity of size and shape of the individuals within each colonial association and the slight differences between different colonies in the same sedimentary layer.

3. Evidence for both living and death processes in the same colony (typical in any living microbial community). The living aspects are demonstrated by: (i) cell division; various stages of cell division (simple diploid fission) were observed ranging from the initial elongation of the cell, formation of a dividing membrane, initial separation of the two halves, almost complete separation with attachment by a "neck" of cell-bound polymer, to complete separation; (ii) chain formation; and (iii) the dislocation of dividing cells, sometimes with better preservation of one half than the other. The death aspects are documented by cell collapse resulting in an outer, wrinkled surface.

4. Association of many individuals with the same morphological characteristics in colonies that may be loosely or densely packed.

5. Association with different types of microorganisms in multispecies colonies or consortia.

6. Association with large amounts of polymer or EPS.

Rods. The size and shape of the rod-shaped organisms are typical for modern microbial rod-shaped organisms (Madigan et al., 2000), as is the evidence for cell division and their association with other structures (coccoids, filaments, and polymer) that are interpreted to be of microbial origin.

EPS. The variability of morphological characteristics of the polymer film (smooth to granular; with holes or cracked; fine films coating sediment particles or thick films embedding monospecies or multispecies colonies; as well as sediment particles) resembles that of modern extracellular polymeric substances (Westall et al., 2000 and references therein). The two types of EPS observed (cell-bound EPS directly linked to the outer walls of the coccoidal cells and EPS that links individual microorganisms in a colony or biofilm) are well known in modern microbial communities.

Colonies and biofilms. The association of many individuals together represents a colony, whether densely packed, as in the "carpet" colonies in Layers 3 and 7, or loosely packed as in the colonies in Layers 4 and 5. At the top of Layer 5 and the base of Layer 6, the totality of all these features, i.e., individuals of different morphologies within an EPS–rich layer that also incorporates sediment particles at a sediment surface, is a typical characteristic of biofilm formation. Moreover, the fact that different types of colonies and biofilms are related to different sedimentary layers supports the interpretation of formation of colonies and biofilms by different species of microorganisms in different microenvironments.

Biogeochemical Signatures

The carbonaceous composition and carbon isotope signal ($\delta^{13}C$ values of around –26‰ to –30‰) are those that would be expected from microorganisms (see discussion of organic carbon content and carbon isotopes below). The high-resolution TEM study showed that, although mature, the kerogens are far from having reached the graphite stage. The structure of the carbon platelets clearly differs from that of pyrocarbons formed by an abiogenic process, such as hydrocarbon decomposition on hot substrates, but is similar to that found in mature kerogens from biological precursors found in the rock-parent of oil (Oberlin, 1989; Skrzypczak et al., 2004).

Environmental Interactions

The coccoidal colonies and multispecies biofilms observed in the "Kitty's Gap Chert" interacted with their immediate environment in a number of ways. In the first place, the coccoidal colonies are distinctly distributed around the edges of the volcanic particles, indicating their specificity for a particular type of substrate. The indications of alteration at the edges of the volcanic clasts, as observed by optical microscopy and analyzed geochemically, coupled with the presence of microbes on the clast surfaces, together suggest that at least part of the alteration process may have been caused by the metabolic activities of the microbes. Thus, part of the supersaturation of silica in the pore waters is probably due to microbial activity, including changes in the pH.

Secondly, the formation of biofilms at the top of Layer 5 and, especially, at the base of Layer 6 greatly influenced the binding of the sediment particles and the stability of the sediment surface. Particles are coated by and at times completely engulfed by EPS that acts as a cement.

Lastly, the presence of the biogenic organic matter on the volcanic particles within the pore spaces of the sediment, as well as at the top of and immediately above a sediment surface, promoted the very early lithification (silicification) process of the whole sediment. The dissolved silica was readily complexed to the organic matter. Functional groups within it and on it acted as initial points of precipitation that led to further polymerization and, finally, contributed to the silicification of the whole sedimentary packet.

We conclude, on the basis of the totality of the microenvironmental, structural, and biogeochemical information and substrate interactions, that the filaments, coccoids, rods, and polymer represent with a high degree of probability the silicified remains of microorganisms, their colonies, and biofilms.

Abiogenic Alternatives

There is at present much debate regarding the origin of the carbonaceous matter in early Archean sediments (see also the discussion on the isotopic signal below) (Brasier et al., 2002; van Zuilen et al., 2002). Metamorphic carbon or keratite (Yushkin, 2000) and laboratory-produced carbon-silica precipitates (Garcia-Ruiz et al., 2003) can mimic certain microbial morphologies. A potential source of abiogenic carbon in the "Kitty's Gap Chert" is the hydrothermal vein that conducted silica-rich fluids into the sediments. However, although such precipitates can imitate individual morphologies, they cannot reproduce the totality of colony or biofilm characteristics exhibited by the mono- and multispecies colonies and biofilms preserved in these silicified sediments, i.e. the regularity in size and shape, the evidence of cell vitality (division), and cell death (collapsed cells), the flexibility of the filamentous forms, the formation of multispecies colonies, the association of EPS (both cell-bound and non–cell-bound), the formation of different types of colonies and biofilms in different microenvironments, the intimate nature of the interactions between the biofilms and their substrate with incorporation of sediment particles, and the carbon isotope signature. We, therefore, exclude the hypothesis that the microstructures described above could be abiogenic artifacts, such as silica spheres or filaments coated with carbon or abiogenic, carbonaceous structures that were subsequently silicified.

In Situ Formation or Later Microbial Contamination

It could be argued that the microorganisms in the "Kitty's Gap Chert" could have infiltrated the rock at a later stage and become fossilized in situ. Westall and Folk (2003) demon-

strated such a situation for the 3.8-Ga-old Isua banded iron formations, in which recent endolithic fungi and cyanobacteria invaded fractures in the rock and were subsequently silicified. Great pains were taken with the "Kitty's Gap Chert" samples to exclude laboratory contamination of the preparations for SEM observation by thorough rinsing in milliQ water and flaming with alcohol during preparation. However, carbon contamination evidently occurred through the handling process of some subsamples, as indicated by the stepped combustion release of carbon at low temperatures in the sample (see discussion below). At the same time, however, the stepped combustion analyses also demonstrate the presence of carbon that is clearly intrinsic to the sample and that is released at high temperatures during stepped combustion. The HR-TEM and Raman spectroscopic evidence for the presence of mature kerogen (Beyssac et al., 2002a, 2002b) in these sediments corroborates the stepped combustion results.

There are a number of lines of evidence demonstrating that the microfossils described above are in situ and that they formed at the same time as the rock. (1) We observe different types of microbial colonies and biofilms in association with different layers representing different microenvironments, which would be difficult to explain if they resulted from field or laboratory contamination. (2) There is also an intimate interrelationship between the biofilms at the base of Layer 6, in Layer 5, and the sediment particulate substrate, with EPS incorporating sediment particles as well as microfossils, which argues for coexistence. (3) The colonies of coccoids are distributed around the edges of the volcanic clasts (Fig. 11) and are not indiscriminately disseminated in the sample, as would be expected if they were contaminants. Their close association with the surfaces of the particles indicates colonization before the silicification and cementation of the rock. (4) Filaments attached to some of the carbonaceous detrital clasts are identical to those observed in association with the biofilm (Figs. 4 and 7). They must have been formed contemporaneously and be very locally derived, otherwise they would have been completely degraded before deposition. Such transported filaments are difficult to explain by contamination. (5) The variability in the level of cellular preservation before silicification also argues for the fact that these organisms must be intrinsic to the rock, for example, the fact that the filaments and coccoids in the biofilm at the base of Layer 6 are more poorly preserved than the colonies of coccoids in the underlying and overlying layers. (6) The microfossils were observed in an etched, cut-rock surface and not on a fracture surface. They were also observed on the surface of a polished thin section, where filaments can be seen traversing the grain boundaries between quartz crystals (Fig. 7F), demonstrating that they must have formed in situ. (7) The maturity of the kerogen (probably biogenic according to the HR-TEM studies) in the "Kitty's Gap Chert" is consistent with the metamorphic grade of the rock (prehnite-pumpellyite), suggesting contemporaneous formation.

We conclude that the microfossils occurring in the "Kitty's Gap Chert" are intrinsic to the rock and are not later infiltrations and that they predated the silicification of the rock.

Microbial Preservation and Timing of Silicification

The microorganisms and their colonies and biofilms have been preserved by silicification, as indicated by the EDX spot and mapping analyses. The process of mineralization must have been relatively rapid because otherwise these delicate, organic structures would not have been preserved. Experimental studies (Westall et al., 1995; Toporski et al., 2002; Orange, 2004) as well as field studies in silica hot springs (de Ronde et al., 2002; Handley, 2004) have shown that the fossilization process can start very rapidly, within hours, and can continue for some days to weeks. The microorganisms in the "Kitty's Gap Chert" exhibit varying degrees of preservation prior to fossilization. A living colony of microorganisms always consists of both living (dividing) and dead (lysed) individuals. In fact, dead cells and EPS are actually more susceptible to fossilization than living cells because of the greater availability of functional groups for complexing mineral species in solution (Westall et al., 2000). Most of the fossilized colonies observed in this sample comprise both living and dead cells. The multispecies biofilm at the base of Layer 6 (fine volcanic dust layer), however, exhibits a higher degree of degradation before fossilization than any of the colonies in the other layers.

Not only are the microorganisms silicified but so is the whole sedimentary sequence. The fact that the microorganisms are preserved at all is evidence that the overall process of silicification was very rapid. The complexation of the silica ions by the organic surfaces of both the EPS as well as the microorganisms must have played an important role in the silicification of this sediment deposit. The silica probably had multiple origins, including (1) silica from the devitrification and diagenetic alteration of the volcanic material, which enriched the pore waters (microbial metabolic activity probably contributed to the process), (2) silica from hydrothermal fluids, and (3) silica in the seawater (*N.B.* until the appearance of microorganisms with siliceous frustules in the Phanerozoic, silica concentrations in the seawater were considerably higher) (see also Orberger et al., this volume). The difference in the state of conservation of microorganisms from different layers, i.e., the relatively well-preserved coccoidal colonies in Layers 3, 4, 5, and 6, as opposed to the relatively poorly preserved biofilm at the base of Layer 6, may be related to differences in SiO_2 concentrations between sediment pore waters and seawater, with the latter being more diluted. The biofilm at the base of Layer 6 may, therefore, have been fossilized at a slower rate than the colonies in the other layers, thus allowing more time for degradation.

The sediments at Kitty's Gap must have been subjected to a number of silicification episodes that were closely spaced in

time: initial silicification of the organic matter and probably penecontemporaneous precipitation of a siliceous cement in the sediments, followed by cross-cutting and bedding-parallel silica veining.

Carbon and Carbon Isotopes as Signatures of Microbial Activity

Carbon Content

Most of the carbon in the "Kitty's Gap Chert" is released at low temperatures from the crushed samples and a smaller amount is released at higher temperatures. As mentioned above (Results section), the uncrushed sample shows, however, a different release pattern: most of the carbon is released at high temperatures with release peaking at 1100 °C. The observation for the uncrushed sample can be explained as a result of the presence of two carbon components: a surface (laboratory) contamination component that is released at low temperatures and a second component that is intrinsic to the sample, released at high temperatures. In the crushed samples, the carbon that is intrinsic to the sample is more easily exposed to oxygen during stepped combustion and, thus, burns at lower temperatures, whereas in the uncrushed sample, oxygen does not come into direct contact with the intrinsic carbon until the temperature is high enough to crack or to melt the sample.

With respect to the concentration of carbon in the sample, we find that the larger the sample aliquot, the lower the measured total carbon concentration is. This implies that contamination is proportional to the sample surface area. The data allow a rough estimation of ~100 ppm for the concentration of the carbon intrinsic to the samples. For the uncrushed sample the amount of intrinsic carbon is 84 ppm.

We can, thus, conclude:

1. The samples contain both laboratory contamination and intrinsic carbon.

2. The combustion temperatures of the two carbon components are similar (200–600 °C).

3. The amount of carbon contamination is comparable with the surface area of each of the subsamples.

The generally low concentrations of carbon in the sample are related to two factors: the low biomass and the silicification of the microorganisms. In terms of weight, the average carbon content in a bacterial cell is $\sim 3.54 \times 10^{-13}$ g. This translates into an even smaller amount of carbon in an individual microfossil because of the effects of degradation and loss of the organic carbon compounds during the mineralization of the cell. Although the numbers of individuals in a colony may reach many hundreds and colonies may be relatively common in the layers of the Kitty's Gap sediments, the overall weight of carbon in a particular layer is diluted by the volcanic components and, especially, the diluting and fossilizing silica. Thus, in a sample with variable microenvironments ranging from pore water spaces containing colonies of microorganisms attached to particle surfaces to sediment surfaces hosting biofilms or mats, there will be heterogeneously distributed pockets with higher concentrations of carbon, although the overall bulk carbon content may be low. In situ analyses of carbon would be the ideal method of analysis and, indeed, would have been successfully used on larger, younger microfossils (e.g., House et al., 2000). However, the ability to measure carbon and carbon isotopes in submicrometer structures is still in the developmental stages.

Carbon Isotopic Compositions

The isotopic compositions of the various layers show that the $\delta^{13}C$ values for the contaminating carbon and the carbon intrinsic to the sample are similar, varying from –22‰ to –30‰ in the combustion steps, with bulk compositions between –25.9‰ and –27.8 ‰. Thus, although in most cases we were not able to distinguish between the contamination and sample carbon, there is strong evidence that the samples contain carbon intrinsic to the sample that has isotopic compositions between –26‰ and –28‰. This result, coupled with the relatively low combustion temperature observed for the carbon (<600 °C), suggests that the intrinsic carbon can be identified with the presence of the microfossils. The HR-TEM observations of probable biogenic kerogen also support this hypothesis.

An alternative explanation for the carbon isotope values is abiogenic fractionation of carbon by Fischer-Tropsch synthesis in hydrothermal systems, since this process can produce an isotopic composition similar to that produced by microbial fractionation (Holm and Charlou, 2001). Although hydrothermal activity was associated with the early diagenetic silicification processes occurring at Kitty's Gap, the overwhelming evidence for microbial colonization in each of the sediment layers investigated suggests that, in this case, the isotope composition of the intrinsic carbon is probably due to microbial fractionation.

Microbial Ecosystems in the Early Archean, Near-Shore, Volcanoclastic Sediments

Subsurface Pore Space: Chemolithotrophic Colonies

The mineralogical substrate on which these microorganisms flourished is volcanic and, according to the protomineralogy, of rhyodacitic composition. The microbial colonies occur around the edges of the pseudomorphosed clasts in Layers 3, 4, and 5, form a biofilm at the top of Layer 5 and at the base of Layer 6, and are mixed in with the fine volcanic dust in Layer 6. The juxtaposition of the colonies with the volcanic material suggests a close relationship between the substrate and microbial metabolism. The coccoidal microfossils may represent at least chemolithotrophic microorganisms that obtained their source of energy from electron donors and acceptors present or extracted from the surfaces of the volcanic particles that they colonized. Their carbon could have come from CO_2 that was abundant in the early Archean environment (Kasting 1993), from organic mole-

cules synthesized on Earth (Nakashima and Shiota, 2001; Russell and Arndt, 2005), or from organic carbon of extraterrestrial origin (Brack et al., 2001; Maurette et al., 2001). In fact, volcanic materials provide a ready source of nutrients for microbes, and studies of recent volcanic glass and pillow basalt surfaces have shown that they are invariably infested by microbes (Ross and Fischer, 1986; Thorseth et al., 1992). The rhyolitic protoliths in the Kitty's Gap sediments would have had fewer nutrients than mafic basalts, but they would still have provided an important source of macronutrients, such as K, as well as minor Fe and some Mg. It is possible that they could have extracted further Mg and Ca from the seawater. Moreover, given the fact that chemolithotrophic microorganisms excrete enzymes to break down the surfaces that they colonize in order to liberate H_2 as an electron donor for their metabolic processes (Brantley et al., 2001), microbial activity may have played a major role in the early diagenetic alteration of the volcanic particles and the liberation of silica.

Sediment Surface: Photosynthesizing Mats?

The boundary between Layers 5 and 6 probably represents a strong change in the energetic regime and a short period of nondeposition. It is at the top of Layer 5 and at the base of Layer 6 that a multispecies biofilm containing filamentous and coccoidal microorganisms formed. It could be hypothesized that some of the microorganisms in the biofilm, such as the filaments, may have been photosynthetic microorganisms, as the biofilm formed conformably on a sediment surface in the photic zone (the overall environment of deposition is a channel-and-flat environment, possibly influenced by tidal activity (de Vries, 2004). The development of photosynthesis (oxygenic or anoxygenic) by the early-mid–Archean has previously been hypothesized (e.g., Walter, 1983; Byerly et al., 1986; Walsh, 1992, 2004; Hofmann et al., 1999; Westall, 2003, 2004; Westall et al., 2001, 2004; Tice and Lowe, 2004). If this were the case for the filaments in the "Kitty's Gap Chert," the photosynthesizing microorganisms must have been anoxygenic, as geochemical studies of the chert (Orberger et al., this volume) indicate that the environment at the time of deposition was anoxic.

Early-Mid–Archean Seawater Temperatures

Knauth and Lowe (2003) noted that the early Archean seawater was probably very warm, >50 °C, if not 80 °C. The microorganisms inhabiting the channel-and-flat sediments at Kitty's Gap may therefore have been mesophilic to thermophilic. de Vries (2004) noted evidence for hydrothermal activity during or immediately after sedimentation. Thus, a contemporaneous influence of warm fluids from hydrothermal venting is a possibility for the Kitty's Gap locality. These warm fluids would have "bathed" the microbial communities and were also a source of the silica in the very early diagenetic silicification processes. The enrichment of Cu and Zn in the darker, finer-grained layers may be a tracer of such hydrothermal fluids (Orberger et al., this volume).

Implication for the Search for Past Traces of Life on Mars

The early Archean volcanoclastic sediments represent suitable analogues for the study of Noachian-age (4.5 to ca. 3.5 Ga) volcanic material on Mars (Westall, 2003, 2004, 2005b; Westall and Walsh, 2003). These sediments were formed at the end of the period when Mars still had liquid water at its surface and in the type of near-shore environment (at the edge of a small basin) that was probably relatively common on Mars. The common occurrence of fossilized colonies of probable chemolithotrophic microorganisms on the surfaces of volcanic clasts in pore spaces and the occurrence of biofilms and mats formed by possible anoxygenic photosynthesizers on the sediment surfaces in the photic zone suggest that a similar situation could have been present on Mars, if life ever arose there. Martian volcanic material could, therefore, be suitable for past life studies.

A recent study of volcanic rock samples concluded that such materials are not suitable for light microscope investigations of microbial biofilms (Walsh, 2004). However, our investigation has shown that volcanic material may be rich in microfossils but, given the submicrometer size range of the organisms and the small sizes of their colonies, highly sophisticated methods of investigation, such as high-resolution scanning electron microscopy, are necessary for their observation (see also Westall, 2005a). The Kitty's Gap microfossils are invisible in thin section because they are intermixed with or embedded by microcrystalline quartz that has the same submicrometer size as the individual organisms themselves (Figs. 12C–12E). Although the submicrometer-sized quartz particles have a definite, angular morphology that distinguishes them from the rounded coccoids in the SEM photomicrographs (Fig. 8), the resolution capabilities in optical microscopy are insufficient to distinguish the shapes of such small particles, whatever their origin. On the other hand, our observations show that the alteration of the volcanic particles in the Kitty's Gap sediments, visible in thin section, may be a telltale indication of microbial activity.

Our study, however, underlines the difficulties involved in making an in situ search for potential microfossil traces in martian rocks: (1) In the first place, sophisticated instrumentation was necessary in order to observe and analyze the signatures of the fossilized microorganisms, although thick accumulations of well-developed microbial biofilms and mats (stromatolites) formed by probable photosynthetic microorganisms can be observed with this method (Walsh, 1992, 2004; Walsh and Lowe, 1999; Tice and Lowe, 2004). Such instrumentation is, at the moment, not miniaturizable for in situ research by a lander/rover on Mars. (2) Secondly, although the microbial colonies are commonly distributed throughout the volcanoclastic sediment, the amount of biogenic organic carbon present in the bulk sediment (or even simply in the individual layers) is very small (0.01%). This means that it would be undetectable with the instrumentation presently designed for future landers/rovers. (3)

Furthermore, it may be difficult to interpret any carbon isotope signal measured in situ. These considerations argue for the return of samples from Mars in order to make a reliable search for life investigation.

CONCLUSIONS

The multidisciplinary approach that we have used, combining detailed environmental, sedimentological, and biogeochemical studies with a high-resolution SEM investigation of microfossils, has proven to be essential for understanding the ancient microcosms present in a 3.446-Ga, volcanoclastic, nearshore, channel-and-flat environment from the Kitty's Gap locality in the Coppin Gap greenstone belt, and our observations have provided a wealth of new information regarding the early Archean microbial habitats. Each millimeter- to centimeter-thick sediment layer formed under slightly different energetic conditions and provided different microenvironments for potential microbial colonization.

The amount of morphological detail made available by the use of the HR-SEMs, together with the environmental and the biogeochemical data, allowed the microstructures to be interpreted, with a high degree of probability, as representing fossilized microorganisms, colonies, and biofilms. Densely packed, "carpet"-like colonies of coccoids having two modal sizes around 0.44 and 0.78 μm colonized the surfaces of the volcanic particles in the pore spaces of Layer 3 and in the fine, volcanic dust in Layer 6; looser colonies of coccoids, many forming chains, occurred on the surfaces of the volcanic shards and mineral debris in the pore spaces of Layers 4 and 5 (modal sizes of 0.4–0.5 and 0.73–0.75 μm). They probably represent chemolithotrophic microorganisms. Biofilms of filaments (width mode 0.35 μm, lengths up to 40 μm), coccoids (modal sizes of 0.4–0.5 and 0.75–0.8 μm), rare rods (0.8 μm in length), and copious quantities of EPS formed at a sediment surface in the photic zone representing a brief period of cessation in sedimentation. The filaments in the biofilms may have been anoxygenic, photosynthetic microorganisms. All the microorganisms may have been mesothermophiles, if the ambient seawater temperatures were as high as estimated (Knauth and Lowe, 2003).

Silicification of the colonies and biofilms was rapid, with the silica originating from supersaturated pore waters owing to the possibly microbially mediated devitrification of the volcanic particles, as well as from hydrothermal and seawater sources. Silicification of the organic matter contributed to silicification of the sediments.

These volcanoclastic sediments with their microfossil communities are an excellent analogue for Noachian-aged rocks on Mars that formed in shallow-water environments. The sophistication of the methods necessary for successful identification of microbial remains precludes in situ search on Mars at current instrumental detection limits, but the knowledge and experience gained about these very ancient terrestrial rocks will be invaluable for the future study of samples returned from Mars.

ACKNOWLEDGMENTS

FW acknowledges the NRC (National Research Council, Washington), JSC (Johnson Space Center, Houston), LPI (Lunar and Planetary Science Institute, Houston), CNRS (Centre National de la Recherche Scientifique, Paris), and CNES (Centre National d'Etudes Spatiales, Paris) for funding made available over the 4 years that these investigations were made. The following people are acknowledged for their technical help: A. Richard (HR-SEM, Orléans) and T. Cacciaguerra and C. Clinard (HR-TEM and Raman spectrometer). VR thanks the French Ministry of Foreign Affairs for supporting his stay at the Planetary Science Laboratory at Osaka University. D. Prieur, M. Walter, and U. Reimold are thanked for their critical comments.

REFERENCES CITED

Allwood, A.C., Walter, M.R., van Kranendonk, M.J., and Kamber, B.S., 2005a, 3.43 Ga stromatolites, rocky shorelines and a carbonate platform: Strelley Pool Chert, Pilbara Craton, Western Australia: NASA Astrobiology Institute Biennial Meeting: Astrobiology, v. 5, no. 2, p. 184.

Allwood, A.C., Walter, M.R., and van Kranendonk, M.J., 2005b, Stromatolite facies of the 3.43 Ga Strelley Pool Chert: Pilbara Craton, Western Australia: NASA Astrobiology Institute Biennial Meeting: Astrobiology, v. 5, no. 2, p. 184.

Beyssac, O., Rouzaud, J.N., Goffe, B., Brunet, F., and Chopin, C., 2002a, Graphitization in a high-pressure, low-temperature metamorphic gradient: A Raman microspectrometry and HRTEM study: Contributions to Mineralogy and Petrology, v. 143, p. 19–31.

Beyssac, O., Goffe, B., Chopin, C., and Rouzaud, J.N., 2002b, Raman spectra of carbonaceous materials in metasediments: A new geothermometer: Journal of Metamorphic Geology, v. 20, p. 859–872, doi: 10.1046/j.1525-1314.2002.00408.x.

Boulmier, J.L., Oberlin, A., Rouzaud, J.N., and Villey, M., 1982, Natural organic matters and carbonaceous materials: A preferential field of application for transmission electron microscopy, *in* O'Hare, A.M.F., ed., Scanning Electron Microscopy: Chicago, SEM Inc., p. 1523–1538.

Brack, A., Barbier, B., Boillot, F., and Chabin, A., 2001, Extraterrestrial organic molecules and the origin of life, *in* Nakashima, S., et al., eds., Geochemistry and the Origin of Life: Tokyo, Universal Academy Press, p. 17–38.

Brantley, S.L., Lierman, L., Bau, M., and Wu, S., 2001, Uptake of trace metals and rare elements from hornblende by a soil bacterium: Geomicrobiology Journal, v. 18, p. 37–61, doi: 10.1080/01490450151079770.

Brasier, M.D., Green, O.R., Jephcoat, A.P., Kleppe, A.K., van Kranendonk, M., Lindsay, J.F., Steele, A., and Grassineau, N., 2002, Questioning the evidence for Earth's oldest fossils: Nature, v. 416, p. 76–81, doi: 10.1038/416076a.

Buick, R., 1990, Microfossil recognition in Archean rocks: An appraisal of spheroids and filaments from a 3500 m.y. old chert-barite unit at North Pole, Western Australia: Palaios, v. 5, p. 441–459.

Byerly, G.R., Walsh, M.M., and Lowe, D.L., 1986, Stromatolites from the 3300–3500 Myr Swaziland Supergroup, Barberton Mountain Land, South Africa: Nature, v. 319, p. 489–491, doi: 10.1038/319489a0.

Cady, S.L., and Farmer, J.D., 1996, Fossilization processes in siliceous thermal springs: Trends in preservation along the thermal gradient, *in* Bock, G.R., et al., eds., Evolution of hydrothermal ecosystems on Earth (and Mars): Chichester, John Wiley, Ciba Symposium 202, p. 150–173.

Cady, S.L., Farmer, J.D., Grotzinger, J.P., Schopf, W.J., and Steele, A., 2003, Morphological biosignatures and the search for life on Mars: Astrobiology, v. 3, p. 351–368, doi: 10.1089/153110703769016442.

Charaklis, W.G., and Wilderer, P.A., eds., 1989, Structure and function of biofilms—Dahlem Workshop report: Chichester, Wiley, 387 p.

de Ronde, C.E.J., Stoffers, P., Garbe-Schönberg, D., Christenson, B.W., Jones, B., Manconi, R., Browne, P.R.L., Hissmann, K., Botz, R., Davy, B.W., Schmitt, M., and Battershill, C.N., 2002, Discovery of active hydrothermal venting in Lake Taupo, New Zealand: Journal of Volcanology and Geothermal Research, v. 115, p. 257–275.

de Vries, S.T., 2004, Early Archean sedimentary basins: Depositional environment and hydrothermal systems: Examples from the Barberton and Coppin Gap greenstone belts: Geologica Ultraiectina: Utrecht, University of Utrecht, 159 p.

DiMarco, M.J., and Lowe, D.R., 1989, Stratigraphy and sedimentology of and early Archean felsic volcanic sequence, eastern Pilbara Block, Western Australia, with special reference to the Duffer Formation and implications for crustal evolution: Precambrian Research, v. 44, p. 147–169, doi: 10.1016/0301-9268(89)90080-6.

Eriksson, K.A., Krapez, B., and Fralick, P.W., 1994, Sedimentology of Archean greenstone belts: Signatures of tectonic evolution: Earth Science Reviews, v. 37, p. 1–88, doi: 10.1016/0012-8252(94)90025-6.

Fedo, C.M., 2000, Setting and origin for problematic rocks from the >3.7 Ga Isua Greenstone Belt, southern west Greenland: Earth's oldest coarse sediments: Precambrian Research, v. 101, p. 69–78, doi: 10.1016/S0301-9268(99)00100-X.

Furnes, H., Banerjee, N.R., Muehlenbachs, K., and Kotninen, A., 2005, Preservation of biosignatures in metaglassy volcanic rocks from the Jormua ophiolite complex, Finland: Precambrian Research, v. 136, p. 125–137, doi: 10.1016/j.precamres.2004.09.009.

Garcia-Ruiz, J.M., Hyde, S.T., Carnerup, A.M., Christy, A.G., van Krankendonk, M.J., and Welham, N.J., 2003, Self-assembled silica-carbonate structures and detection of ancient microfossils: Science, v. 302, p. 1194–1197, doi: 10.1126/science.1090163.

Handley, K.M., 2004, *In situ* experiments on the growth and textural development of subaerial microstromatolites, Champagne Pool, Waiotapu, New Zealand [M.S. thesis]: Auckland, University of Auckland, 111 p.

Hickman, A.H., 1983, Geology of the Pilbara Block and its environs, Western Australia: Geological Survey Bulletin, v. 127, 268 p.

Hickman, A.H., 1990, Excursion no. 5: Pilbara and Hammersley Basin, *in* Ho, S.E., et al., eds., Excursion guidebook, Third International Archean Symposium, Perth, 1990: University of Western Australia, Geology Department External Services, v. 21, p. 1–58.

Hofmann, H.J., Gray, K., Hickman, A.H., and Thorpe, R.I., 1999, Origin of 3.45 Ga coniform stromatolites in Warrawoona Group, Western Australia: Geological Society of America Bulletin, v. 111, p. 1256–1262.

Holm, N.G., and Charlou, J.L., 2001, Initial indicators of abiogenic formation of hydrocarbons in the Rainbow ultramafic hydrothermal system, Mid-Atlantic Ridge: Earth and Planetary Science Letters, v. 191, p. 1–8, doi: 10.1016/S0012-821X(01)00397-1.

House, C.H., Schopf, J.W., McKeegan, K.D., Coath, C.D., Harrison, T.M., and Stetter, K.O., 2000, Carbon isotopic composition of Precambrian microfossils: Geology, v. 28, p. 707–710.

Kasting, J.F., 1993, Earth's early atmosphere: Science, v. 259, p. 920–926.

Kisch, H.J., and Nijman, W., 2004, Metamorphic grade from the K-micas in the metasediments from the Pilbara and Barberton greenstone belts, *in* Reimold W.U., and Hofmann, A., eds., Field Forum on Processes on the Early Earth, Kaapvaal Craton, South Africa: Johannesburg, University of Witwatersrand, p. 47–48.

Knauth, L.P., and Lowe, D.R., 2003, High Archean climatic temperature inferred from oxygen isotope geochemistry of cherts in the 3.5 Ga Swaziland Supergroup, South Africa: Geological Society of America Bulletin, v. 115, p. 566–580, doi: 10.1130/0016-7606(2003)115<0566:HACTIF>2.0.CO;2.

Krumbein, W.E., Paterson, D.M., and Stal, L.J., eds., 1994, Biostabilization of sediments: Oldenburg, Biblioteks und Informationssystem der Carl von Ossietzky Universität, 526 p.

Levitt, G.S., and Krumbein, W.E., 2003, Is there and adequate terminology of biofilms and microbial mats?, *in* Krumbein, W.E., et al., eds., Fossil and Recent Biofilms: Amsterdam, Kluwer, p. 333–341.

Lowe, D.R., 1994, Abiological origin of described stromatolites older than 3.2 Ga: Geology, v. 22, p. 287–290.

Madigan, M.T., Martinko, J.M., and Parker, J., eds., 2000, Brock: Biology of Microorganisms: Upper Saddle River, New Jersey, Prentice Hall, 991 p.

Maurette, M., Matrajt, G., Gounelle, M., Engrand, C., and Duprat, J., 2001, La matière extraterrestre primitive et les mystères de nos origines, *in* Gargaud, M., et al., eds., Éléments d'exobiologie: L'environnement de la Terre primitive et l'origine de la vie: Bordeaux, Presses University of Bordeaux, p. 99–127.

McGregor, V.R., and Mason, B., 1977, Petrogenesis and geochemistry of metabasaltic and metasedimentary enclaves in the Amitsoq gneisses: West Greenland: American Mineralogist, v. 62, p. 887–904.

McKay, D.S., Gibson, E.K., Thomas-Keprta, K., Vali, H., Romanek, C.S., Clemett, S.J., Chillier, X.D.F., Maechling, C.R., and Zare, R.N., 1996, Search for past life on Mars: Possible relic biogenic activity in Martian meteorite ALH84001: Science, v. 273, p. 924–930.

Monty, C.L.V., Westall, F., and van der Gaast, S.T., 1991, Diagenesis of siliceous particles in subantarctic sediments, ODP Leg 114, Hole 699A: Possible microbial mediation, *in* Ciesielski, P.F., et al., eds., Proceedings ODP Scientific Results, 114: College Station, Texas, Ocean Drilling Program, p. 685–710.

Nakashima, S., and Shiota, D., 2001, Organic-inorganic interactions and the origin and evolution of life, *in* Nakashima, S., et al., eds., Geochemistry and the Origin of Life: Tokyo, Universal Academy Press, p. 135–177.

Nijman, W., Willigers, B.J.A., and Krikke, A., 1999, Tensile and compressive growth structures: Relationships between sedimentation, deformation and granite intrusion in the Archean Coppin Gap greenstone belt, Eastern Pilbara, Western Australia: Precambrian Research, v. 95, p. 277–302, doi: 10.1016/S0301-9268(99)00013-3.

Oberlin, A., 1989, High resolution TEM studies of carbonization and graphitization, *in* Thrower, P.A., ed., Chemistry and Physics of Carbon: New York, Marcel Dekker, v. 22, p. 1–143.

Orange, F., 2004, Expériences de silicification de bactéries extrêmophiles: Application à la recherche de signatures de vie dans les roches primitives et extra-terrestres [M.S. thesis]: Orléans, University of Orléans, 33 p.

Orberger, B., Rouchon, V., Westall, F., de Vries, S.T., Pinti, D.L., Wagner, C., Wirth, R., and Hashizume, K., 2006, this volume, Microfacies and origin of some Archean cherts (Pilbara, Australia), *in* Reimold, W.U., and Gibson, R.L., Processes on the early Earth: Geological Society of America Special Paper 405, 10.1130/2006.2405(08).

Pflug, H.D., 1979, Archean fossil finds resembling yeasts: Geologie und Palaeontologie, v. 13, p. 1–8.

Pflug, H.D., 2001, Earliest organic evolution, essay to the memory of Bartholomew Nagy: Precambrian Research, v. 106, p. 79–92, doi: 10.1016/S0301-9268(00)00126-1.

Pflug, H.D., and Jaeschke-Boyer, H., 1979, Combined structural and chemical analysis of 3,800-Myr-old microfossils: Nature, v. 280, p. 483–486, doi: 10.1038/280483a0.

Robbins, E.I., 1987, *Appelella ferrifera,* a possible new iron-coated microfossil in the Isua Iron-Formation, southwestern Greenland, *in* Appel, P.W.U., et al., eds., Precambrian Iron Formations: Athens, Theophrastes, p. 141–154.

Rosing, M.T., 1999, 13C depleted carbon microparticles in >3700 Ma seafloor sedimentary rocks from West Greenland: Science, v. 283, p. 674–676, doi: 10.1126/science.283.5402.674.

Ross, K.A., and Fischer, R.V., 1986, Biogenic grooving on glass shards: Geology, v. 14, p. 571–573, doi: 10.1130/0091-7613(1986)14<571:BGOGS>2.0.CO;2.

Rouchon, V., and Orberger, B., Westall, F., Gallien, J.-P., and Pinti, D.L., 2004a, Archean protominerals and their evolution during chert formation: Kittys Gap, Pilbara Complex: Goldschmidt Conference: Abstracts, Geochimica et Cosmochimica Acta, v. 68 (11S), p. A-751.

Rouchon, V., Sugihara A., Orberger, B., Pinti, D.L., Hashizume, K., Gallien, J.P., Westall, F., 2004b, Using nuclear probe and mass spectrometry to constrain the nitrogen composition of an early Archean chert: The Mass Spectrometry Society of Japan Abstracts, Yamagata, 24–26 November 2004.

Rouchon, V., Pinti, D.L., Gallien, J.P., Orberger, B., Daudin, L., and Westall, F., 2005, NRA analyses of N and C in hydromuscovite aggregates from a 3.5 Ga chert from Kittys Gap, Pilbara, Australia: Nuclear Methods and Instruments in Physics Research, v. B231, p. 536–540.

Rouzaud, J.N., and Clinard, C., 2002, Quantitative high resolution transmission electron microscopy: A promising tool for carbon materials characterization: Fuel Processing Technology, v. 77–78, p. 229–235, doi: 10.1016/S0378-3820(02)00053-X.

Russell, M., and Arndt, N., 2005, Geodynamic and metabolic cycles in the Hadean: Biogeosciences, v. 2, p. 97–111.

Schopf, J.W., 1993, Microfossils of the early Archean Apex Chert: New evidence of the antiquity of life: Science, v. 260, p. 640–646.

Schopf, J.W., and Packer, B.M., 1987, Early Archean (3.3-billion- to 3.5-billion-year-old) microfossils from Warrawoona Group, Australia: Science, v. 237, p. 70–73.

Schopf, J.W., and Walter, M.R., 1983, Archean microfossils: New evidence of ancient microbes, *in* Schopf, J.W., ed., Earth's Earliest Biosphere: Princeton, Princeton University Press, p. 214–239.

Schopf, J.W., Kudryavtsvev, A.B., Agresti, D.G., Wdowiak, T.J., and Czaja, A.D., 2002, Laser-Raman imagery of Earth's earliest fossils: Nature, v. 416, p. 73–76, doi: 10.1038/416073a.

Skrzypczak, A., Derenne, S., Robert, F., Binet, L., Gourier, D., Rouzaud, J.-N., and Clinard, C., 2004, Characterization of the organic matter in an Archean chert (Warrawoona, Australia): Lunar and Planetary Science Conference Abstracts XXXV, no. 1241.

Stal, L.J., 1994, Microbial mats: Ecophysiological interactions related to biogenic sediment stabilization, *in* Krumbein, W.E., et al., eds., Biostabilization of Sediments: Oldenburg, Biblioteks und Informationssystem der Carl von Ossietzky Universität, p. 41–54.

Thorseth, I.H., Furnes, H., and Heldal, M., 1992, The importance of microbiological activity in the alteration of natural basaltic glass: Geochimica et Cosmochimica Acta, v. 56, p. 845–850, doi: 10.1016/0016-7037(92)90104-Q.

Tice, M., and Lowe, D.R., 2004, Photosynthetic microbial mats in the 3,416-Myr-old ocean: Nature, v. 431, p. 549–552, doi: 10.1038/nature02888.

Toporski, J.K.W., Westall, F., Thomas-Keprta, K.A., Steele, A., and Mckay, D.S., 2002, The simulated silicification of bacteria—New clues to the modes and timing of bacterial preservation and implications for the search for extraterrestrial microfossils: Astrobiology, v. 2, p. 1–26, doi: 10.1089/153110702753621312.

Van Kranendonk, M.J., Hickman, A.H., Smithies, R.H., Nelson, D.R., and Pike, G., 2002, Geology and tectonic evolution of the Archean North Pilbara Terrain, Pilbara Craton, Western Australia: Economic Geology and the Bulletin of the Society of Economic Geologists, v. 97, p. 695–732.

van Zuilen, M., Lepland, A., and Arrhenius, G., 2002, Reassessing the evidence for the earliest traces of life: Nature, v. 418, p. 627–630, doi: 10.1038/nature00934.

van Zuilen, M., Lepland, A., Teranes, J., Finarelli, J., Wahlen, M., and Arrhenius, G., 2003, Graphite and carbonates in the 3.8 Ga old Isua Supracrustal Belt, southern West Greenland: Precambrian Research, v. 126, p. 331–348, doi: 10.1016/S0301-9268(03)00103-7.

Verchovsky, A.B., Sephton, M.A., Wright, I.P., and Pillinger, C.T., 2002, Separation of planetary noble gas carrier from bulk carbon in enstatite chondrites during stepped combustion: Earth and Planetary Science Letters, v. 199, p. 243–255, doi: 10.1016/S0012-821X(02)00592-7.

Walsh, M.M., 1992, Microfossils and possible microfossils from the early Archean Onverwacht Group, Barberton Mountain Land, South Africa: Precambrian Research, v. 54, p. 271–293, doi: 10.1016/0301-9268(92)90074-X.

Walsh, M.M., 2004, Evaluation of early Archean volcanoclastic and volcanic flow rocks as possible sites for carbonaceous fossil microbes: Astrobiology, v. 4, p. 429–437, doi: 10.1089/ast.2004.4.429.

Walsh, M.M., and Lowe, D.R., 1999, Modes of accumulation of carbonaceous matter in the early Archaean: A petrographic and geochemical study of carbonaceous cherts from the Swaziland Supergroup, *in* Lowe, D.R., and Byerly, G.R., eds., Geologic evolution of the Barberton greenstone belt, South Africa: Geological Society of America Special Paper 329, p. 115–132.

Walter, M.R., 1983, Archean stromatolites: Evidence of the Earth's earliest benthos, *in* Schopf, J.W., ed., Earth's Earliest Biosphere: Princeton, Princeton University Press, p. 187–213.

Westall, F., 1997, The influence of cell wall composition on the fossilization of bacteria and the implications for the search for early life forms, *in* Cosmovici, C.B., et al., eds., Astronomical and Biochemical Origins and the Search for Life in the Universe: Bologna, Editrici Compositori, p. 491–504.

Westall, F., 1999, The nature of fossil bacteria: Journal of Geophysical Research, Planets, v. 104, p. 16,437–16,451, doi: 10.1029/1998JE900051.

Westall, F., 2003, Stephen Jay Gould, les procaryotes et leur évolution dans le contexte géologique: Palevol, v. 2, p. 485–501, doi: 10.1016/j.crpv.2003.09.009.

Westall, F., 2004, Early life on earth: The ancient fossil record, *in* Ehrenfreund, P., et al., eds., Astrobiology: Future Perspectives: Dordrecht, Kluwer, p. 287–316.

Westall, F., 2005a, Life on the early Earth: A sedimentary view: Science, v. 308, p. 366–367, doi: 10.1126/science.1107227.

Westall, F., 2005b, The geological context for the origin of life and the mineral signatures of fossil life, *in* Martin, H., et al., eds., The Early Earth and the Origin of Life: Berlin, Springer, p. 195–219.

Westall, F., and Folk, R.L., 2003, Exogenous carbonaceous microstructures in early Archean cherts and BIFs from the Isua greenstone belt: Implications for the search for life in ancient rocks: Precambrian Research, v. 126, p. 313–330, doi: 10.1016/S0301-9268(03)00102-5.

Westall, F., and Rincé, Y., 1994, Biofilms, microbial mats and microbe-particle interactions: Electron microscope observations from diatomaceous sediments: Sedimentology, v. 41, p. 147–162.

Westall, F., and Walsh, M.M., 2003, Fossil biofilms and the search for life on Mars, *in* Krumbein, W.E., et al., eds., Fossil and Recent Biofilms: Amsterdam, Kluwer, p. 447–465.

Westall, F., Boni, L., and Guerzoni, M.E., 1995, The experimental silicification of microbes: Palaeontology, v. 38, p. 495–528.

Westall, F., Steele, A., Toporski, J., Walsh, M., Allen, C., Guidry, S., Gibson, E., Mckay, D., and Chafetz, H., 2000, Polymeric substances and biofilms as biomarkers in terrestrial materials: Implications for extraterrestrial samples: Journal of Geophysical Research, Planets, v. 105, p. 24,511–24,527, doi: 10.1029/2000JE001250.

Westall, F., De Wit, M.J., Dann, J., Van Der Gaast, S., de Ronde, C., and Gerneke, D., 2001, Early Archean fossil bacteria and biofilms in hydrothermally influenced, shallow water sediments, Barberton greenstone belt, South Africa: Precambrian Research, v. 106, p. 93–116, doi: 10.1016/S0301-9268(00)00127-3.

Westall, F., Orberger, O., Rouchon, V., Rouzaud, J.-N., and Wright, I., 2004, On the identification of early Archaean microfossils in cherts from Barberton and the Pilbara, *in* Reimold, U.W., and Hofmann, A., comp., Abstract volume, Field Forum on Processes on the Early Earth, Kaapvaal craton, 4–9 July, 2004: Johannesburg, University of the Witwatersrand, p. 94–97.

Williams, I.R., 1990, Geology of the Muccan: Western Australia Geological Survey, Geological Series Explanatory Notes, scale 1:100,000, 39 p.

Wright, I.P., and Pillinger, C.T., 1989, Carbon isotopic analysis of small samples by use of stepped-heating extraction and static mass spectrometry, *in* Shanks, W.C., and Criss, R.E., eds., New Frontiers in Stable Isotopic Research: Laser Proves, Ion Probes, and Small-Sample Analysis: U.S. Geological Survey Bulletin, v. 7890, p. 9–34.

Yushkin, N.P., 2000, Biomineral homologies, organismobiosis, and the problem of biomarkers, *in* Hoover, R.B., ed., Instruments, Methods, and Missions for Astrobiology III, Proceedings of SPIE, the International Society for Optical Engineering, 4137, p. 22–35.

Manuscript Accepted by the Society 4 October 2005

Printed in the USA

Geological Society of America Special Papers

The 3.466 Ga "Kitty's Gap Chert," an early Archean microbial ecosystem

Frances Westall, Sjoukje T. de Vries, Wouter Nijman, et al.

Geological Society of America Special Papers 2006;405; 105-131
doi:10.1130/2006.2405(07)